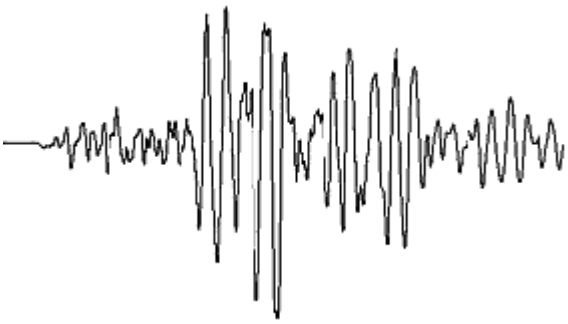

The November 14, 2007 M7.7 Northern Chile Earthquake – Fun with Filtering [1]

Larry Braile
Professor, Purdue University
braile@purdue.edu
http://web.ics.purdue.edu/~braile/
November, 2007

1. Objectives: Illustrate the use of filtering of seismograms to learn more about earthquakes and wave propagation in the Earth and better understand the characteristics of signals contained in seismograms. Sometimes, filtering a seismogram is similar to searching for clues, like being a detective, to try to determine what happened to produce the signals observed on the seismogram!

2. Introduction: There are several interesting features of seismograms from the November 14, 2007 M7.7 Northern Chile earthquake that can be revealed by filtering the seismograms. The November 14, 2007 seismogram recorded on the WLIN AS-1 station is shown in Figure 1 (AmaSeis 24-hour screen display).

This document is available for viewing with a browser (html file) and for downloading as an MS Word document or PDF file at the following locations:
http://web.ics.purdue.edu/~braile/edumod/as1lessons/filtering/filtering.htm
http://web.ics.purdue.edu/~braile/edumod/as1lessons/filtering/filtering.doc
http://web.ics.purdue.edu/~braile/edumod/as1lessons/filtering/filtering.pdf

[1] Explorations in Earth Science

Last modified December 26, 2007

The web page for this document is:
http://web.ics.purdue.edu/~braile/edumod/as1lessons/filtering/filtering.htm
Partial funding for this development provided by the National Science Foundation.

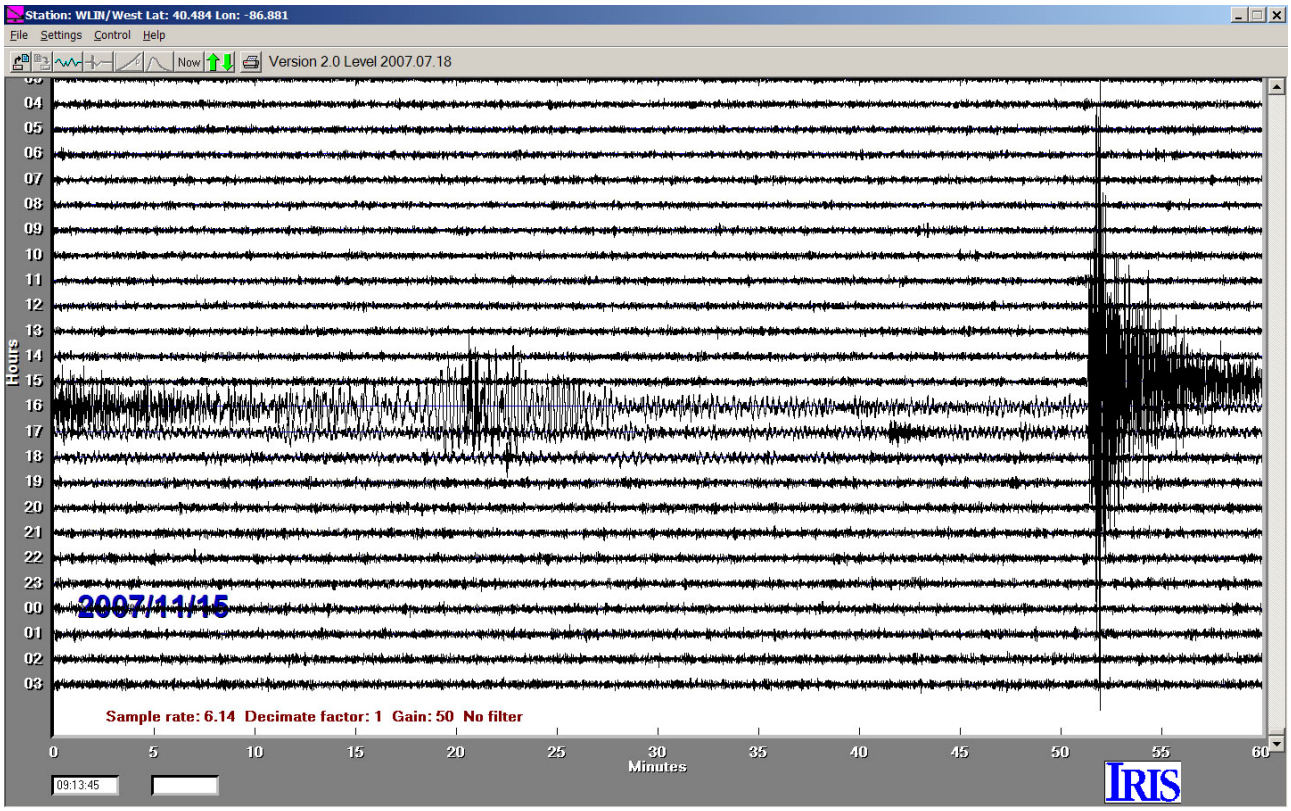

Figure 1. AmaSeis 24-hour screen display for November 14-15, 2007 the WLIN AS-1 station showing the record of the M7.7 Northern Chile earthquake.

Data and a summary map from the USGS (http://earthquake.usgs.gov) for this event and some aftershocks are given in Figures 2 and 3, and the WLIN event data for the N. Chile earthquake are shown in the Table given in Figure 4.

3. Analysis of the WLIN Northern Chile Seismogram: The WLIN seismogram (Figure 5) displays a very prominent P-wave arrival and smaller amplitude, approximately 20 second period surface waves that begin about 26 minutes later. No other easily discernible arrivals (phases) are visible on the raw seismogram. However, one can see some unusual high-frequency energy within the surface waves (Figure 6). Applying a high pass filter (0.5 Hz cutoff frequency) to the seismogram (to reduce the long period surface waves), a separate high frequency arrival is recognized (Figure 7). This energy arrives about 29 minutes after the P arrival.

When I first saw the high frequency arrival on the seismogram (Figures 6 and 7), I thought that it probably was from an aftershock and that, because it occurred a short time after the M7.7 earthquake, it hadn't yet been identified and located. A day or two later, the suspected aftershock still had not shown up on the USGS earthquake list, so I started looking at some other seismograms (both AS-1 records available on SpiNet and some global network records downloaded using the IRIS WILBER tool). There were several potential aftershock signals on these seismograms in the approximate time range of the high frequency arrival on the WLIN seismogram. I tried picking the arrival times of the suspected aftershock arrivals on several seismograms and locating the event using standard earthquake location techniques. Nothing worked very well, so I went back to the original WLIN record and considered other options for the source of the high frequency arrival.

Because the arrival shows up on the WLIN record and other seismograms, it is possible that the arrival is a later arriving phase from the Northern Chile earthquake.

The arrival time of the high frequency phase on the WLIN seismogram closely matched the expected time for the PKPPKP phase – a raypath that travels from the earthquake focus through the Earth's mantle and outer core and reflects off the surface on the far side of the Earth and then travels again through the mantle and outer core finally arriving at a station within about 90 degrees distance from the earthquake epicenter (an illustration will be provided later in this discussion). Because the match of travel time for this phase at only a single station is not very convincing evidence for identifying any unknown arrival, I examined other seismograms from large earthquakes in the range of zero to 90 degrees from the WLIN station to try to confirm that the high frequency arrival was actually the PKPPKP phase.

Update time = Fri Nov 16 9:47:11 UTC 2007

	MAG	UTC DATE-TIME y/m/d h:m:s	LAT deg	LON deg	DEPTH km	Region
MAP	5.4	2007/11/16 08:42:43	-22.489	-70.298	35.0	OFFSHORE ANTOFAGASTA, CHILE
MAP	5.3	2007/11/16 07:52:22	-5.537	151.726	45.3	NEW BRITAIN REGION, PAPUA NEW GUINEA
MAP	6.7	2007/11/16 03:13:00	-2.304	-77.793	119.0	PERU-ECUADOR BORDER REGION
MAP	5.8	2007/11/15 17:18:23	-22.842	-175.199	40.1	TONGA REGION
MAP	5.6	2007/11/15 15:15:49	-22.641	-70.162	28.4	ANTOFAGASTA, CHILE
MAP	6.8	2007/11/15 15:06:01	-22.881	-70.067	35.0	ANTOFAGASTA, CHILE
MAP	6.2	2007/11/15 15:03:09	-22.813	-70.314	27.0	OFFSHORE ANTOFAGASTA, CHILE
MAP	5.0	2007/11/15 11:14:51	-23.175	-70.766	26.9	OFFSHORE ANTOFAGASTA, CHILE
MAP	5.0	2007/11/15 08:53:46	6.081	126.806	84.0	MINDANAO, PHILIPPINES
MAP	5.0	2007/11/15 01:46:35	-23.181	-70.515	14.3	ANTOFAGASTA, CHILE
MAP	5.0	2007/11/14 18:55:49	-22.736	-70.350	31.5	OFFSHORE ANTOFAGASTA, CHILE
MAP	5.3	2007/11/14 18:47:53	-11.526	166.205	63.3	SANTA CRUZ ISLANDS
MAP	5.7	2007/11/14 17:44:04	-23.215	-70.526	38.1	ANTOFAGASTA, CHILE
MAP	5.3	2007/11/14 17:35:41	13.741	-90.773	54.8	OFFSHORE GUATEMALA
MAP	5.0	2007/11/14 17:18:46	-23.147	-70.008	46.1	ANTOFAGASTA, CHILE
MAP	7.7	2007/11/14 15:40:50	-22.178	-69.809	40.0	ANTOFAGASTA, CHILE
MAP	5.0	2007/11/14 14:37:12	31.195	141.744	26.6	IZU ISLANDS, JAPAN REGION
MAP	5.0	2007/11/14 10:37:20	-1.856	99.508	35.0	KEPULAUAN MENTAWAI REGION, INDONESIA
MAP	5.4	2007/11/14 04:29:55	1.500	127.085	99.6	HALMAHERA, INDONESIA

Figure 2. USGS earthquake list (http://earthquake.usgs.gov/eqcenter/recenteqsww/Quakes/quakes_big.php) November 14-16, 2007.

4. The PKPPKP Phase on WLIN Seismograms: I found several WLIN seismograms from large earthquakes (a large event is needed as the PKPPKP phase has a very long travel path compared to the direct P arrival and thus has much smaller amplitude, as seen in Figure 7) in the appropriate distance range. I high-pass filtered the seismograms and measured the difference in travel times between the PKPPKP and the first P arrivals and compared these times with theoretical times calculated from a standard Earth velocity model. Three of the additional seismograms are shown in Figures 8, 9 and 10. Additional information on filtering AS-1 seismograms (or other sac-file records) with the AmaSeis software can be found in Section 3.5 of the Using AmaSeis tutorial: http://web.ics.purdue.edu/~braile/edumod/as1lessons/UsingAmaSeis/UsingAmaSeis.htm.

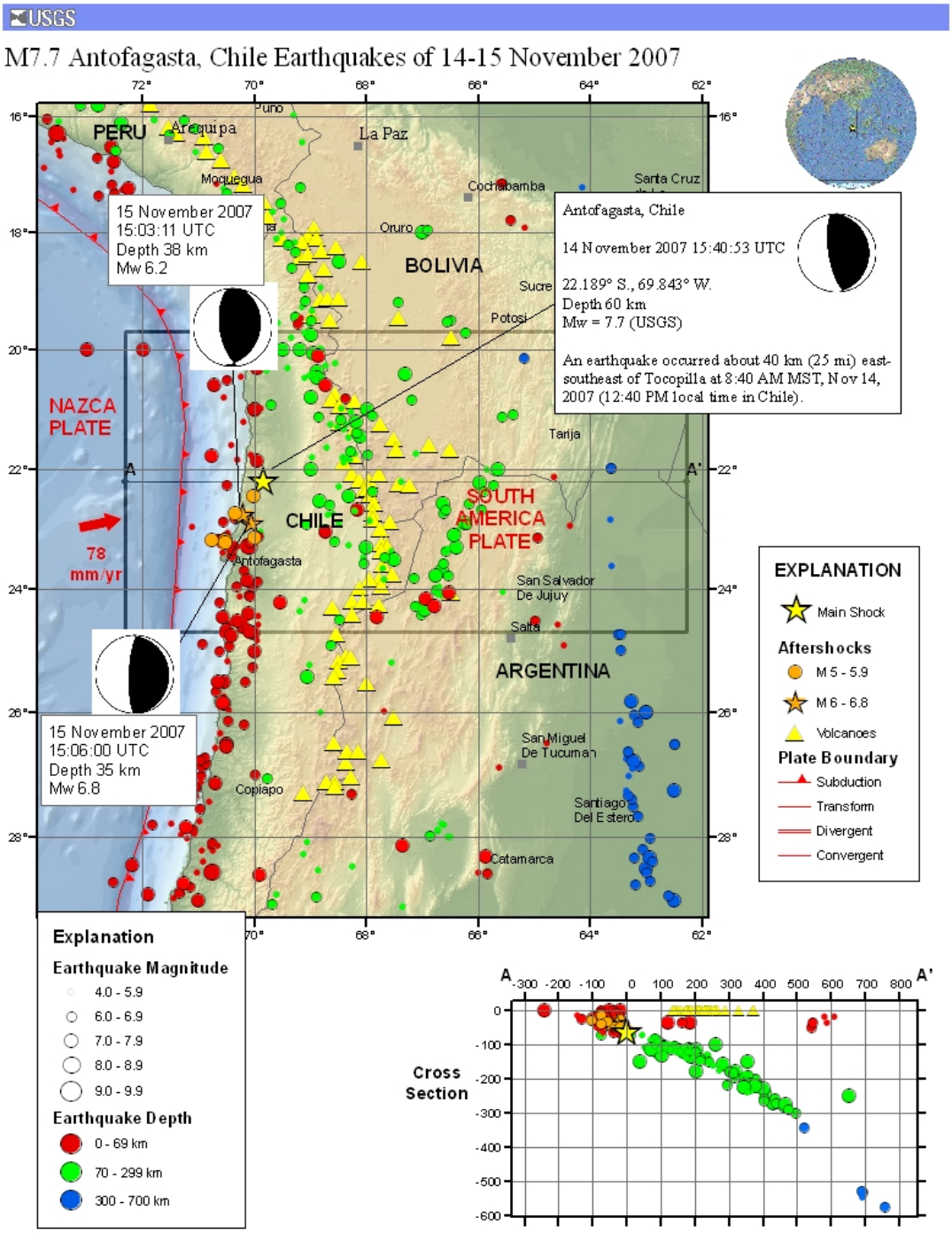

Figure 3. USGS summary map and information for the M7.7 Northern Chile earthquake (http://earthquake.usgs.gov/eqcenter/eqinthenews/2007/us2007jsat/#summary).

Earthquake List - Events recorded, WLIN AS-1 Seismograph (40.484N, 86.881W, 205 m), West Lafayette, Indiana (L. Braile)														
DATE	TIME(GMT)	LAT	LON	DEP.	USGS	USGS	USGS	USGS	AS-1	AS-1	AS-1	Calc. Dist	AS-1 Dist	Location
YY/MM/DD	HR:MN:SS	Deg.	Deg.	(km)	mb	MS	Mw	mbLg	mb	MS	mbLg	Deg.	Deg.	
07/11/14	15:40:53	-22.178	-69.809	40	6.8	7.4	7.7		6.6	7.1		64.330	64.6	N. Chile, Antofagasta

Figure 4. WLIN station information for November 14, 2007 Northern Chile earthquake.

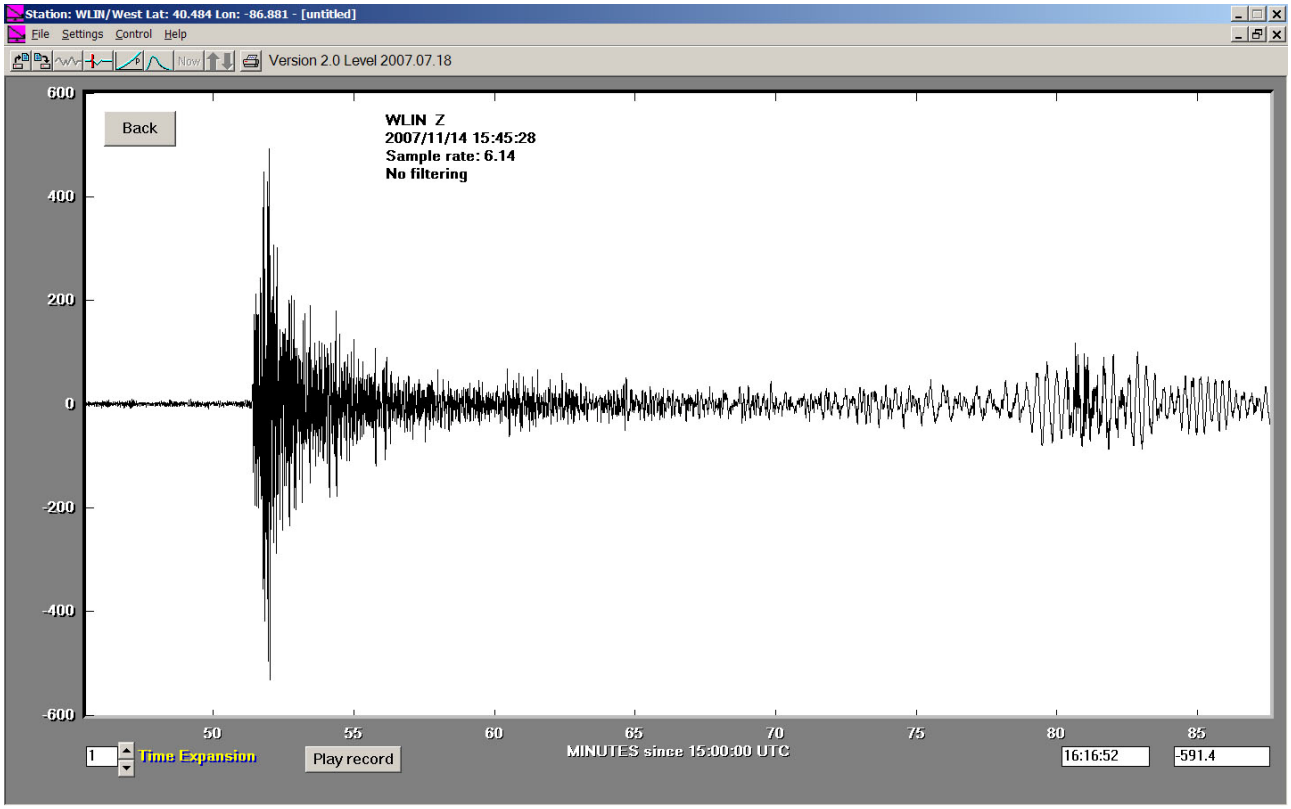

Figure 5. AmaSeis seismogram display for November 14, 2007 the WLIN AS-1 station showing the seismogram of the M7.7 Northern Chile earthquake (http://web.ics.purdue.edu/~braile/edumod/as1lessons/filtering/0711141552WLIN.sac).

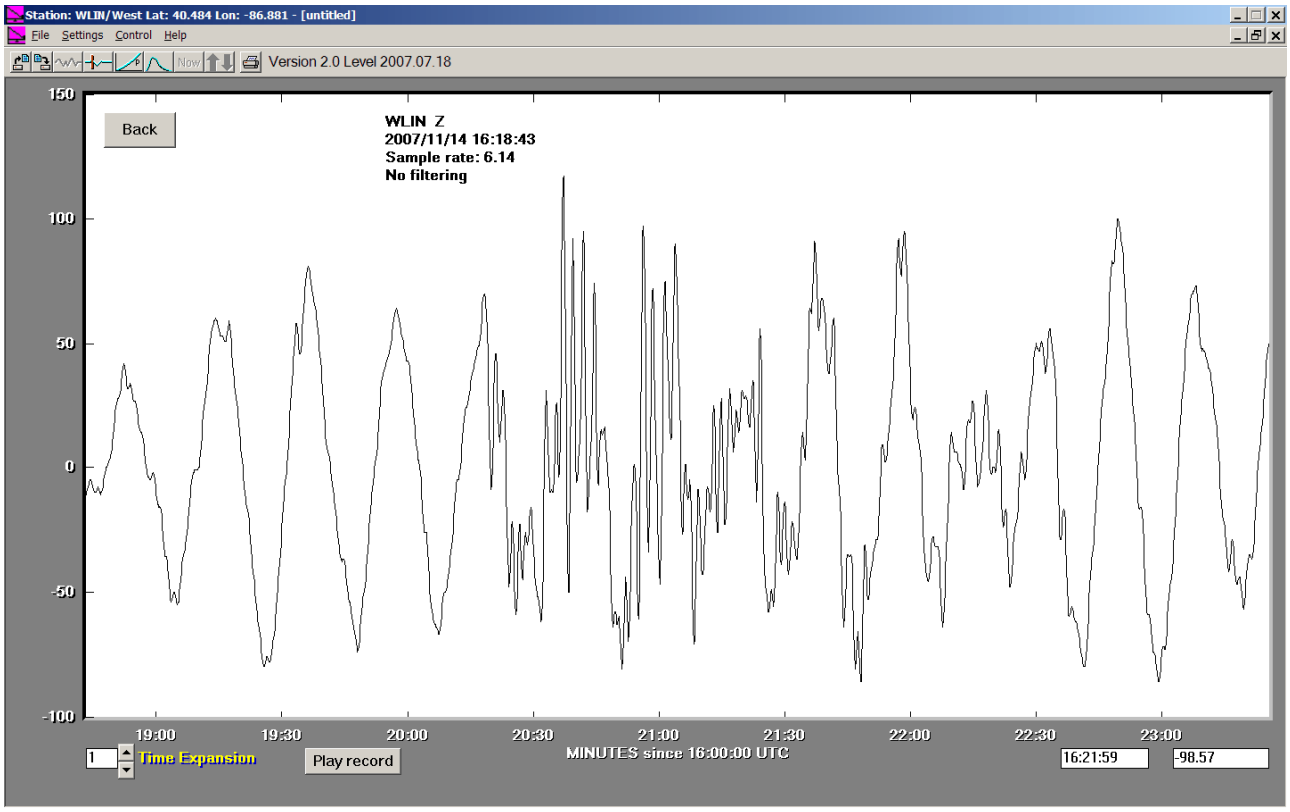

Figure 6. Close-up view of the surface wave arrival. Note the "unusual" high frequency energy.

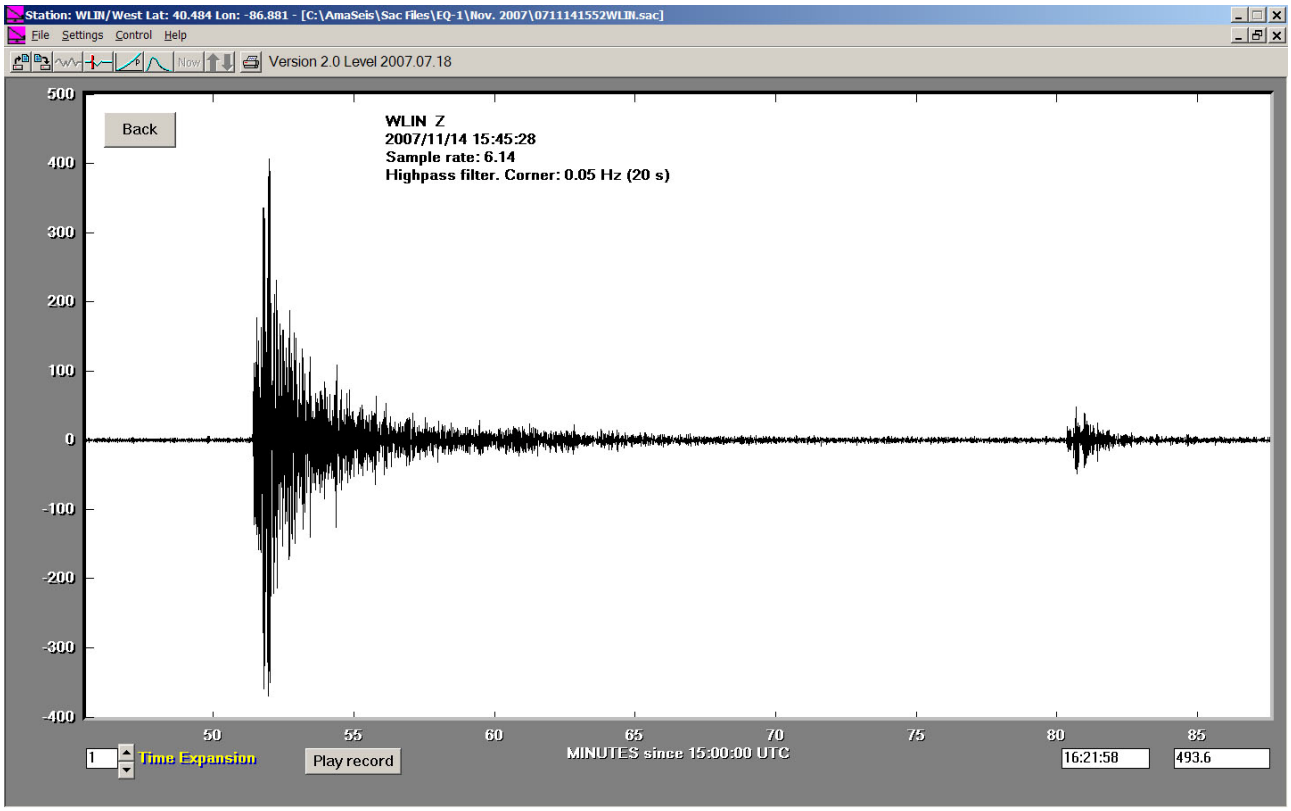

Figure 7. High pass filtered (0.5Hz) seismogram of the M7.7 Northern Chile earthquake.

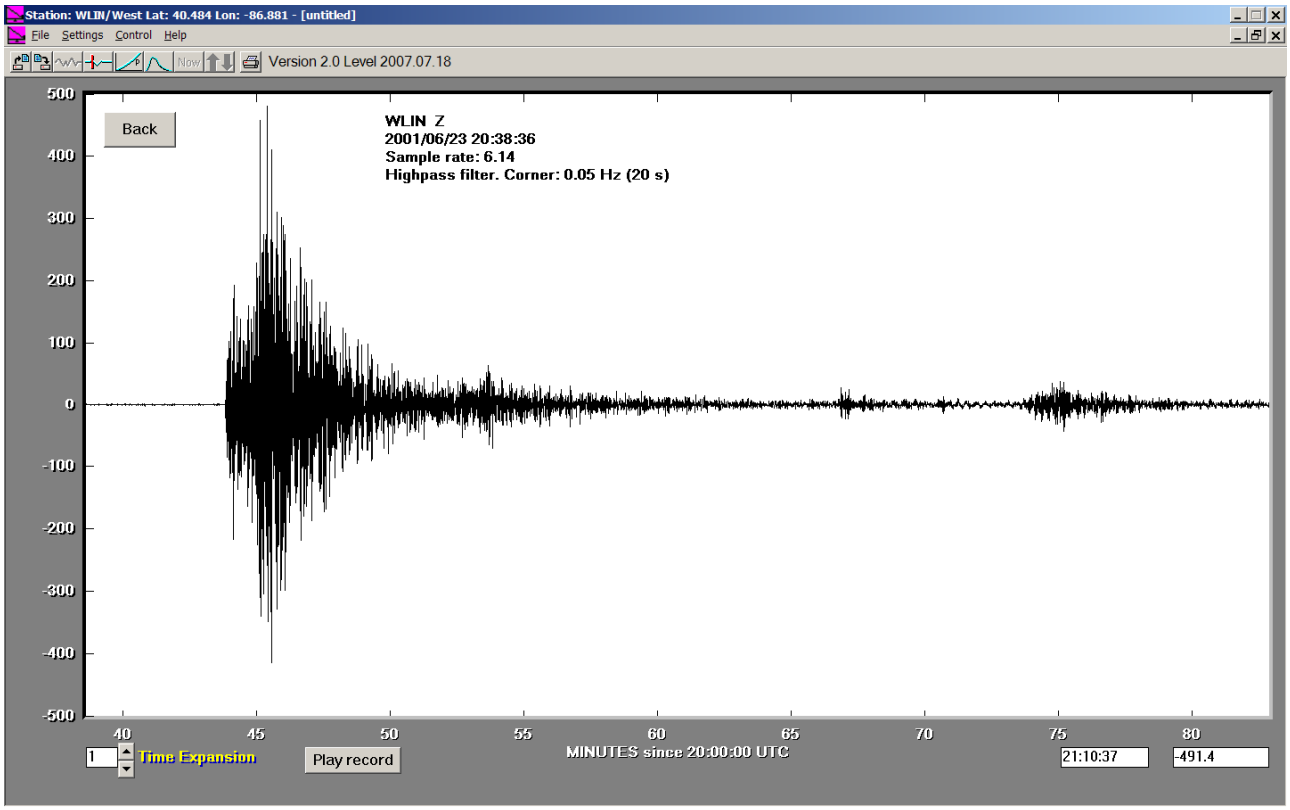

Figure 8. High pass filtered (0.5Hz) seismogram of the M8.4 June 23, 2001 Peru earthquake.

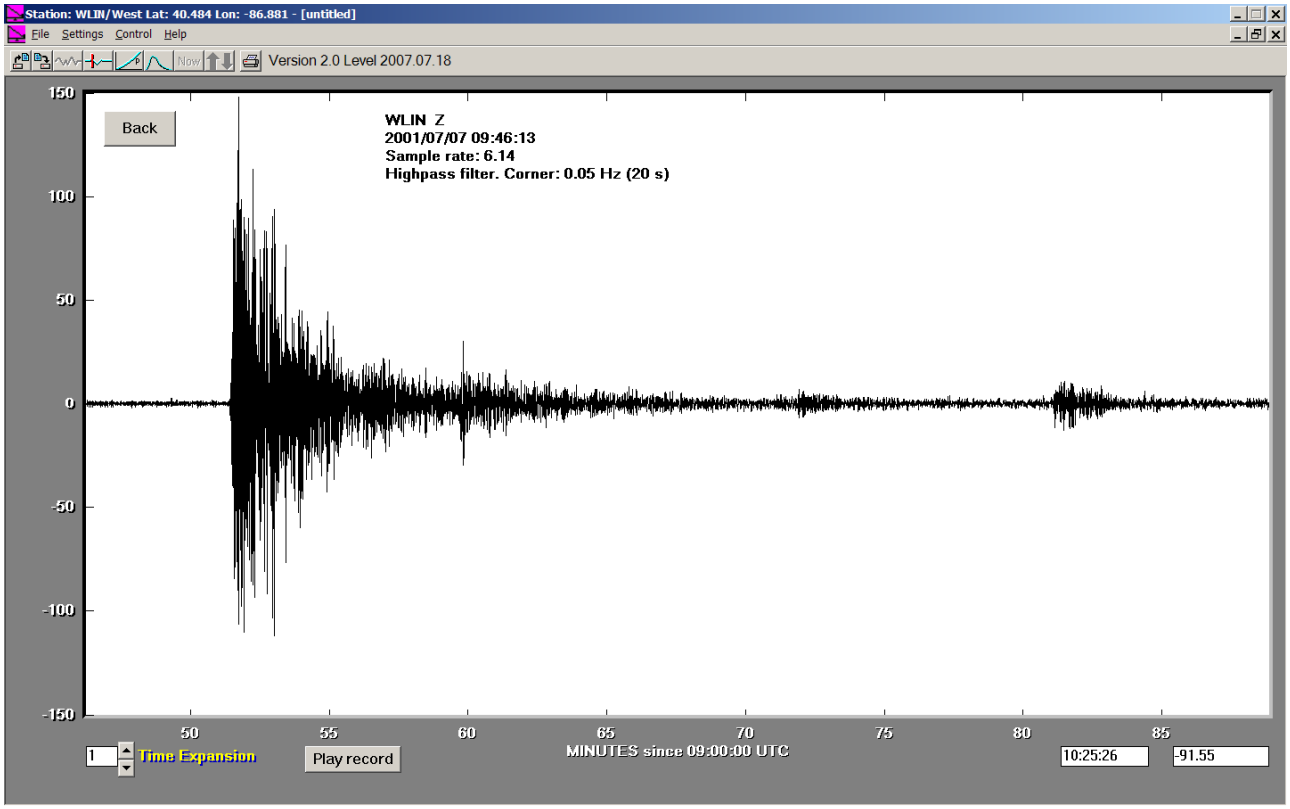

Figure 9. High pass filtered (0.5Hz) seismogram of the M7.6 July 7, 2001 Peru earthquake.

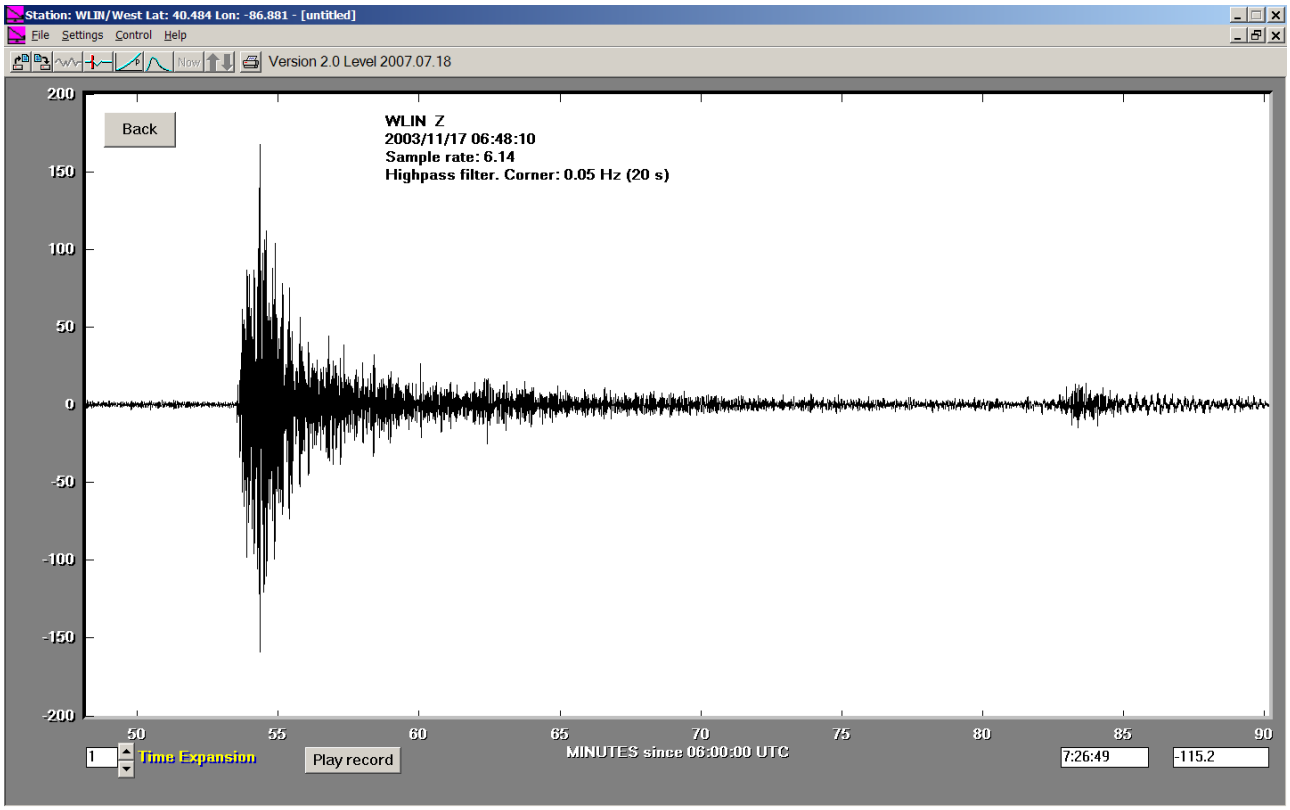

Figure 10. High pass filtered (0.5Hz) seismogram of the M7.8 November 17, 2003 Aleutian Islands earthquake.

The event information for the selected WLIN PKPPKP seismograms is shown in the table in Figure 11. A comparison of the observed and calculated PKPPKP minus P travel times for nine WLIN seismograms is given in the table in Figure 12. Links to the seismograms (sac format) are given in the table in Figure 13. The close match between the observed and calculated times for seismograms from a significant range of distances confirms the identification of the PKPPKP phase as the source of the high frequency energy arriving about 25-31 minutes after the first P arrival in these seismograms. The travel time relationship for the P and PKPPKP phases is illustrated in the travel time curves in Figure 14. I also analyzed the seismograms from AS-1 stations AZAZ, SHCA and VVNY (obtained from SpiNet - http://www.scieds.com/spinet/) and found that the observed PKPPKP-P travel times matched the theoretical times to within a few seconds. Note that as the distance increases, the PKPPKP minus P travel time decreases (Figure 12). This travel time relationship is similar to a few other phases represented on the travel time curves in Figure 14, and results from the PKPPKP phase initially "going the opposite direction" or "taking the long way" to the station. We will also see this effect later when we further examine the surface wave arrival. The raypath for the PKPPKP phase is illustrated in Figure 15.

Note that to confirm the identification of the PKPPKP phase, we needed to analyze more than one seismogram. However, the phase was visible on individual seismograms through a simple filtering process available using the AmaSeis software.

1	Earthquake List - Events recorded, WLIN AS-1 Seismograph (40.484N, 86.881W, 205 m), West Lafayette, Indiana (L. Braile)															
2	DATE	TIME(GMT)	LAT	LON	DEP.	USGS	USGS	USGS	USGS	AS-1	AS-1	AS-1	Calc. Dist	AS-1 Dist	Location	Comments
3	YY/MM/DD	HR:MN:SS	Deg.	Deg.	(km)	mb	MS	Mw	mbLg	mb	MS	mbLg	Deg.	Deg.		X = lost data
4	00/05/12	18:43:18	-23.550	-66.450	225	6.2		7.2		6.5			66.480	65.3	Argentina	Int. depth, P,pP,PP,S
5	01/06/23	20:33:14	-16.265	-73.641	33	6.7	8.2	8.4		6.5	7.7		57.740		Near coast of Peru	Good complete seismogram
6	01/07/07	9:38:44	-17.543	-72.077	33	6.6	7.3	7.6		6.5	6.8		59.310	68.3	Near coast of Peru	
7	02/06/28	17:19:30	43.770	130.720	564	6.8		7.3		7.2			89.540		E Russia -NE China Bor.	
8	03/09/25	19:50:07	41.827	143.830	33	6.9	8.1	8.3		6.5	7.8		86.070		Off co. Hokkaido, Japan	Largest event last 2 1/2 yrs
9	03/11/17	6:43:06	51.146	178.650	33	6.2	7.2	7.8		6.4	7.2		62.300		Aleutian Islands	
10	05/09/26	1:55:38	-5.678	-76.398	115	6.7		7.5		6.7			46.930	46.1	N. Peru	
11	07/01/13	4:23:21	46.243	154.524	10	7.3	8.2	8.1		7.3	8.1		77.750		E of Kuril Islands	
12	07/11/14	15:40:53	-22.178	-69.809	40	6.8	7.4	7.7		6.6	7.1		64.330	64.6	N. Chile, Antofagasta	Good S and SS (LP filtered)

Figure 11. Table of earthquake information for WLIN PKPPKP seismograms.

Event Num.	DATE YY/MM/DD	USGS Mw	Calc. Dist Deg.	Location	PKPPKP minus P Time Observed (mn:ss)	PKPPKP minus P Time Calculated (mn:ss)
1	05/09/26	7.5	46.93	N. Peru	**31:56**	**31:54**
2	01/06/23	8.4	57.74	Near coast of Peru	**29:53**	**29:48**
3	01/07/07	7.6	59.31	Near coast of Peru	**29:36**	**29:35**
4	03/11/17	7.8	62.30	Aleutian Islands	**29:15**	**29:10**
5	07/11/14	7.7	64.33	N. Chile, Antofagasta	**29:00**	**28:51**
6	00/05/12	7.2	66.48	Argentina	**28:31**	**28:35**
7	07/01/13	8.1	77.75	E of Kuril Islands	**27:09**	**27:06**
8	03/09/25	8.3	86.07	Off co. Hokkaido, Japan	**26:08**	**26:07**
9	02/06/28	7.3	89.54	E Russia -NE China Bor.	**25:42**	**25:44**

Figure 12. Table of travel times for WLIN PKPPKP seismograms. The information is sorted by increasing epicenter-to-station distance (given in degrees geocentric angle). Observation of PKPPKP at smaller distances is more difficult because of the small number of large events within about 45 degrees of WLIN. An explanation of distances measured in geocentric angle is available in the Interpreting Seismograms tutorial at:
http://web.ics.purdue.edu/~braile/edumod/as1lessons/InterpSeis/InterpSeis.htm.

Event	Seismogram

Num.	
1	http://web.ics.purdue.edu/~braile/edumod/as1lessons/filtering/0509260204WLIN.sac
2	http://web.ics.purdue.edu/~braile/edumod/as1lessons/filtering/0106232043WLIN.sac
3	http://web.ics.purdue.edu/~braile/edumod/as1lessons/filtering/0107070952WLIN.sac
4	http://web.ics.purdue.edu/~braile/edumod/as1lessons/filtering/0311170653WLIN.sac
5	http://web.ics.purdue.edu/~braile/edumod/as1lessons/filtering/0711141552WLIN.sac
6	http://web.ics.purdue.edu/~braile/edumod/as1lessons/filtering/0005121853WLIN.sac
7	http://web.ics.purdue.edu/~braile/edumod/as1lessons/filtering/0701130435WLIN.sac
8	http://web.ics.purdue.edu/~braile/edumod/as1lessons/filtering/0309252003WLIN.sac
9	http://web.ics.purdue.edu/~braile/edumod/as1lessons/filtering/0206281732WLIN.sac

Figure 13. Table of links for sac files for PKPPKP seismograms. The event numbers correspond to the list in the Table in Figure 12. To use, download the seismograms into a folder (name it "N. Chile EQ Activity" or a name of your choice) within the AmaSeis folder on your computer.

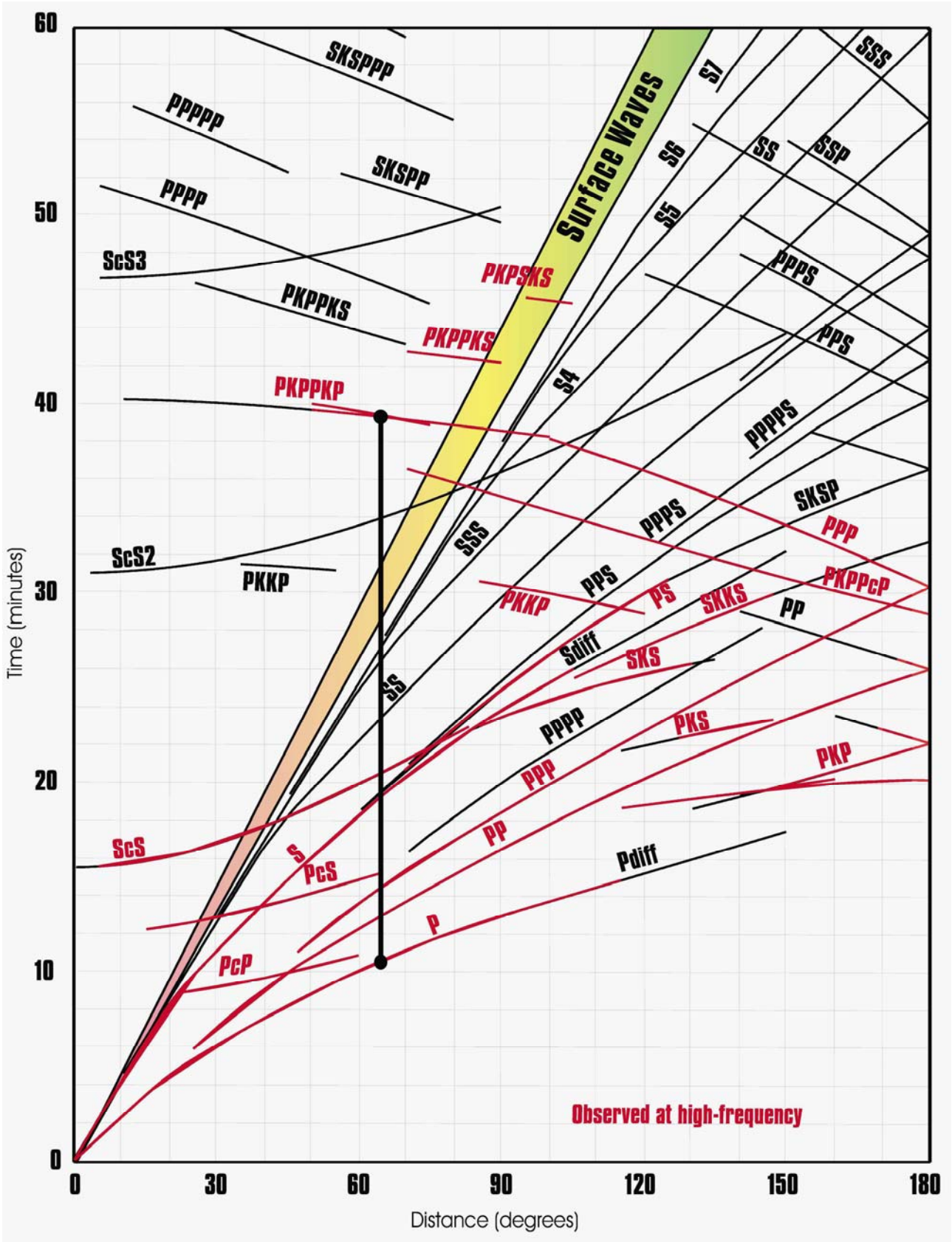

Figure 14. Standard travel-time curves (http://neic.usgs.gov/neis/travel_times/) for various phases (arrivals) for the Earth. The dots show travel times for the N. Chile WLIN seismogram for the P and PKPPKP arrivals. The vertical line shows the PKPPKP – P travel time difference.

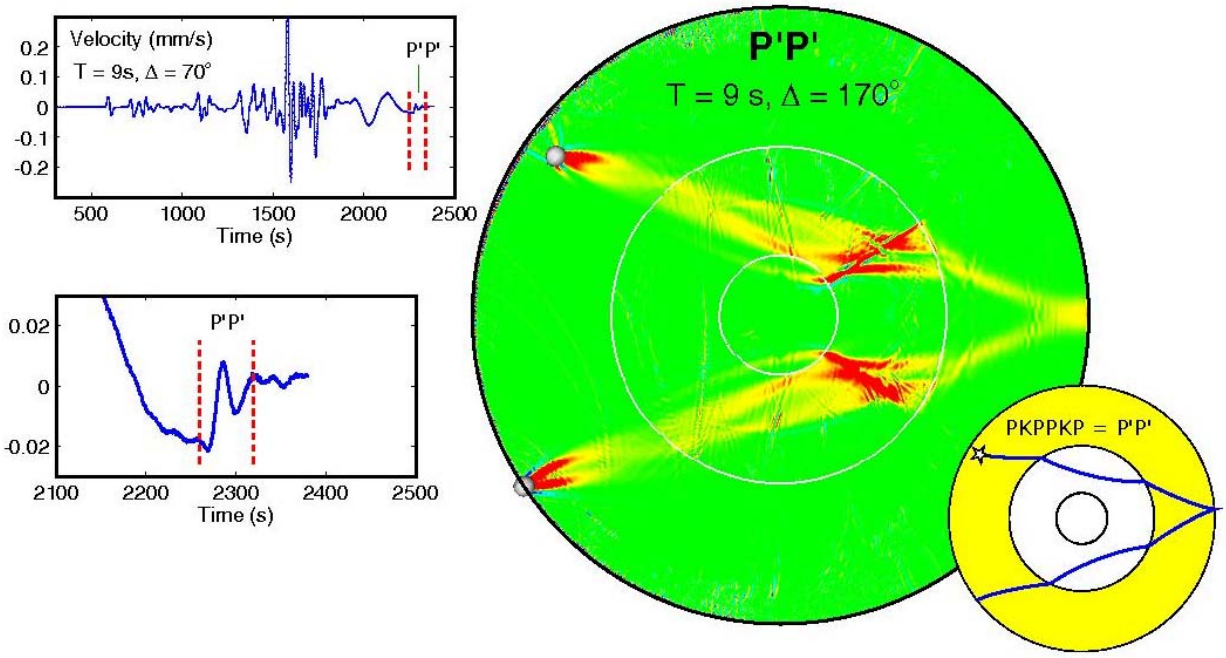

Figure 15. Illustration of the PKPPKP phase (also called P'P'). The seismograms show a weak long-period PKPPKP arrival calculated from a standard Earth velocity model. The large Earth cross section illustrates the complex raypaths (from the calculated numerical model) of the wave energy that contributes to the PKPPKP phase arrival. The small Earth cross section shows the simplified PKPPKP raypath. Note that the P phase would travel more directly from the earthquake (the star in the small Earth cross section) to the recording station (in this example, about 60 degrees from the epicenter).
(from: http://www.agu.org/focus_group/SEDI/main/images/PKPPKP.html)

5. Calculating the Magnitude of the Northern Chile Earthquake from the WLIN Seismogram: The epicenter-to-station distance for the N. Chile earthquake was 64.33 degrees. Measuring the maximum amplitude of the P arrival in about the first 15 seconds of the wave energy (Figure 16) yields a value of 212 digital units. The wave energy has a period of about 2 seconds. Entering these values into the online AS-1 Magnitude Calculator, MagCalc, (http://web.ics.purdue.edu/~braile/edumod/MagCalc/MagCalc.htm) results in an mb magnitude of 6.6. Entering the same data, as well as the depth of 40 km, into the AmaSeis mb magnitude tool produces an mb magnitude value of 6.9. The official USGS mb magnitude (an average of estimates from 182 seismograph stations) is 6.8. We can also calculate the surface wave magnitude (MS) from the maximum amplitude of the approximately 20-second period surface wave energy (visible in Figure 6; to enhance the surface wave and reduce the high frequency arrival, one can filter the seismogram with a low-pass filter with a 10 second cutoff period). The measured amplitude is 81 digital units and results in an MS magnitude of 7.1 using either MagCalc or the AmaSeis MS magnitude tool. The USGS MS magnitude (an average of estimates from 198 seismograph stations) is 7.4. Additional information on magnitude calculation from AS-1 seismograms can be found in Section 3.7 of the Using AmaSeis tutorial:
http://web.ics.purdue.edu/~braile/edumod/as1lessons/UsingAmaSeis/UsingAmaSeis.htm.

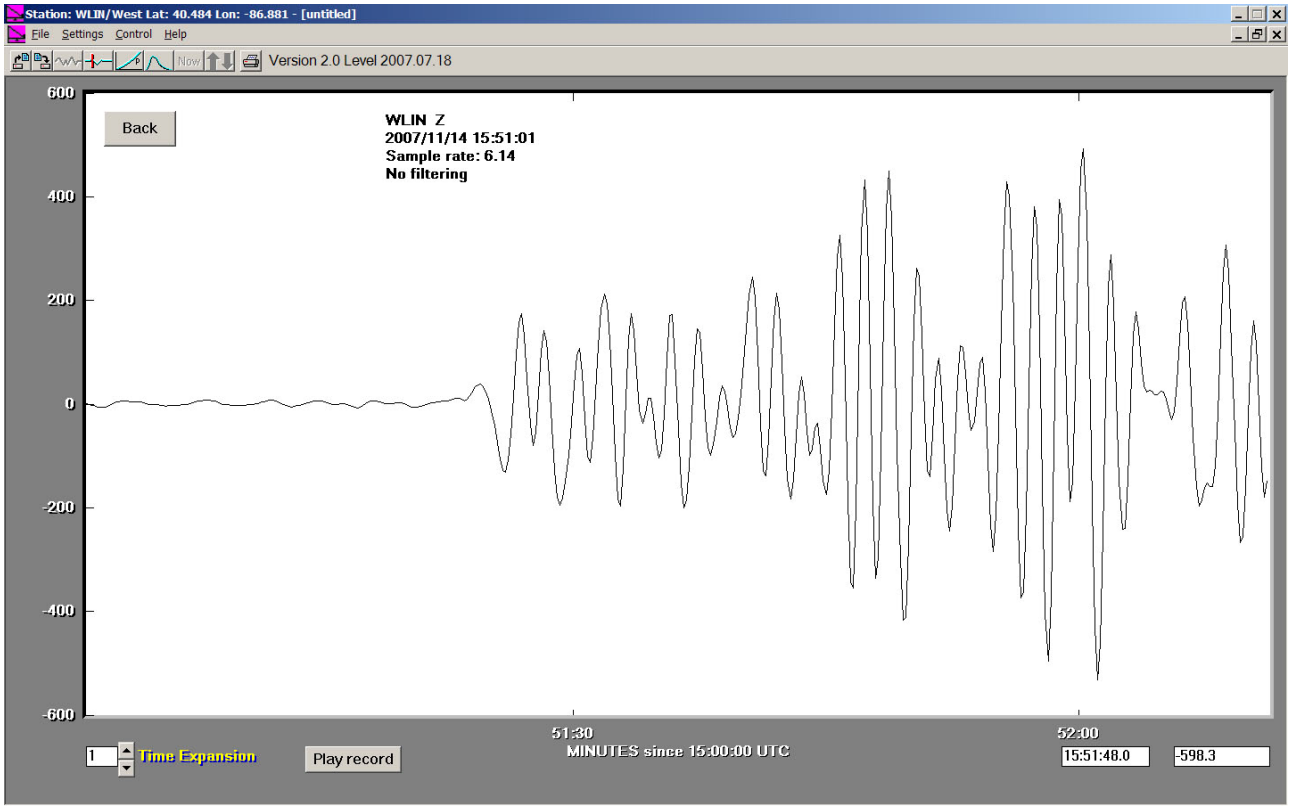

Figure 16. Close-up view of the P-arrival for the N. Chile earthquake.

6. Identification of the S Arrival and Estimating the Epicenter-to-Station Distance from the S Minus P Time: The S minus P travel time method can be used to estimate the epicenter-to-station distance from a seismogram for earthquakes within about 110 degrees from the station. An S minus P earthquake location exercise is available at: http://web.ics.purdue.edu/~braile/edumod/as1lessons/EQlocation/EQlocation.htm. Identification of the S arrival on AS-1 vertical component seismograms is sometimes difficult or impossible. However, for regional or more distant events, low-pass filtering the seismogram with a cutoff frequency of 0.5 Hz (2 s period) or 0.2 Hz (5 s period) often allows the S arrival to be recognized. Another filter in AmaSeis that is often effective is the "long period filter" developed by Bob McClure. Applying the long period filter (settings are: Natural Frequency/Period = 2 s, Q = 0.707, LP = 20 s) to the N. Chile WLIN seismogram (Figure 5) results in the filtered seismogram shown in Figure 17. Note the prominent arrival (recognized by large amplitude and a shift in frequency of the wave energy (to lower frequencies) at a time of about 60 minutes past 15:00 on the time scale. The surface wave energy is also enhanced by this filter.

Using the arrival time picking tool in AmaSeis, one can select the arrival times of the P and S waves on the filtered seismogram and then use the travel time curve tool to estimate the epicenter-to-station distance as shown in Figure 18. When the seismogram is displayed in the travel time curve window, one can use the mouse cursor to move the seismogram on the screen until the P and S arrival times correspond to the first blue (direct P) and green (direct S) curves. The epicenter-to-station distance determined by the S minus P time for the N. Chile seismogram is ~64.6 degrees in good agreement with the distance calculated by using the latitudes and longitudes of the station and epicenter. This calculation can be made in AmaSeis if the epicenter coordinates are entered using

the Event dialog box under the Settings pull-down menu, or by using the USGS online travel time calculation tool (http://neic.usgs.gov/neis/travel_times/).

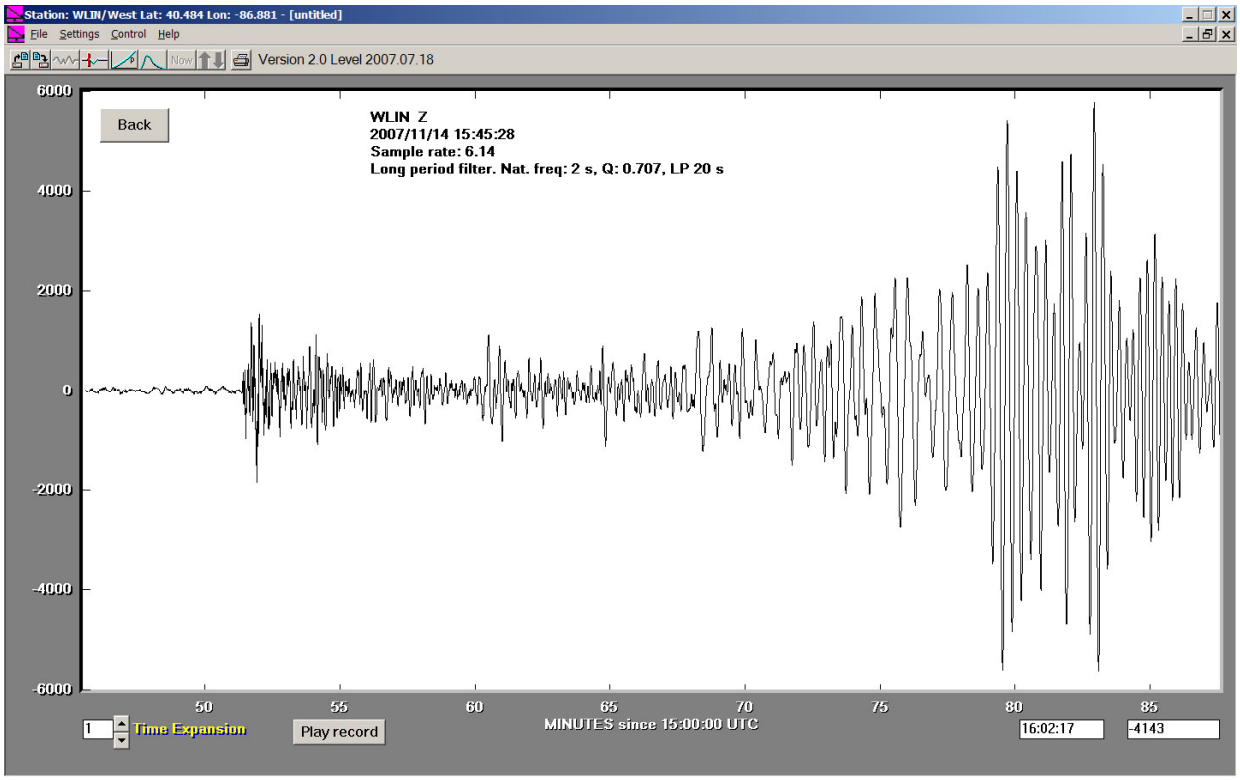

Figure 17. Long-period filtered seismogram of the M7.7 Northern Chile earthquake.

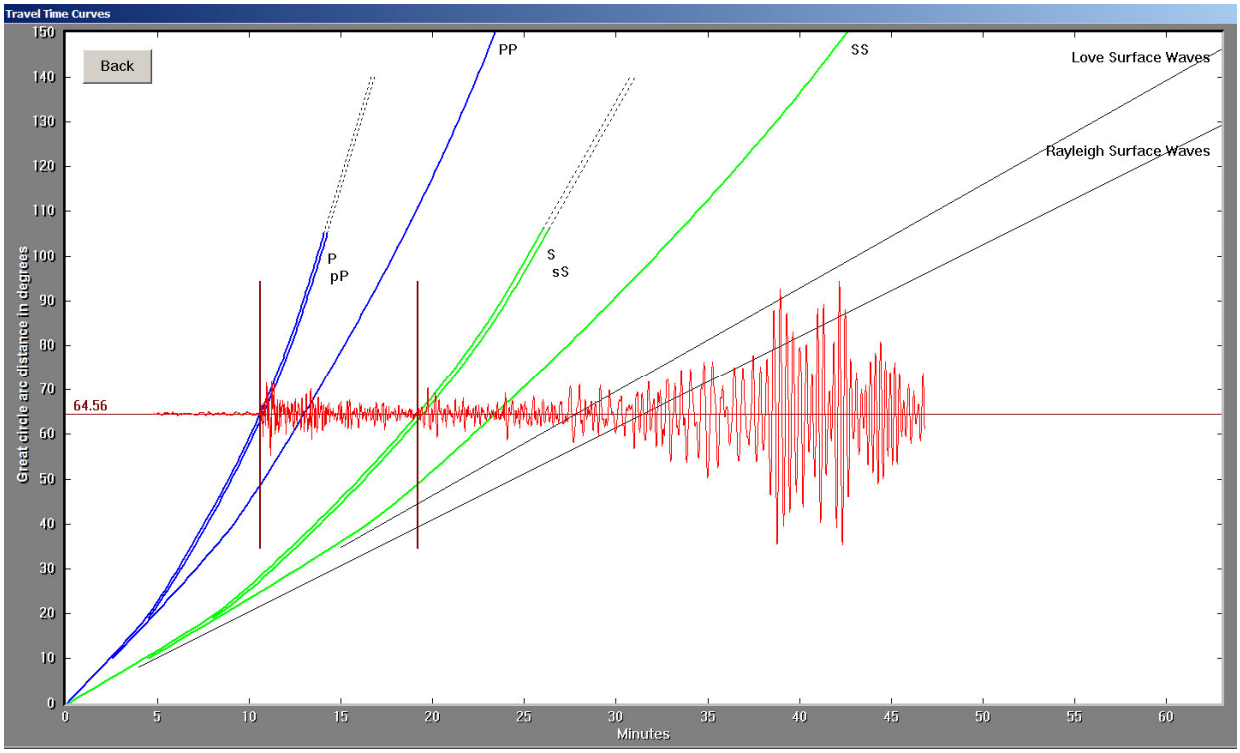

Figure 18. Long-period filtered seismogram displayed using the AmaSeis travel time curve tool.

7. Surface Waves Around the World: In the process of examining the WLIN N. Chile seismogram to see if there were aftershocks visible after high-pass filtering (see section 3 above), I extracted a long (~ 3 hour) seismogram for analysis (Figure 19). Two aftershocks and a separate event (from Guatemala; see earthquake list in Figure 2) were visible on the high-pass filtered seismogram. As expected, the most prominent features of the 3-hour seismogram (Figure 19) are the P arrival and the surface waves beginning about 26 minutes after the first P energy. After low-pass filtering (three times) with the long period filter available in AmaSeis, the surface waves are enhanced and additional ~20 s period energy is visible about 125 minutes after the large-amplitude surface waves (Figure 20). This ~20 s period energy is also surface waves that have traveled "the long way" around the Earth (about 296 degrees) to reach the WLIN seismograph station. These late-arriving surface waves have much smaller amplitude than the earlier surface waves due to the greater distance traveled. An very effective illustration of surface waves that travel around the world is given in the IRIS poster for the December 26, 2004 Sumatra earthquake (Figure 21).

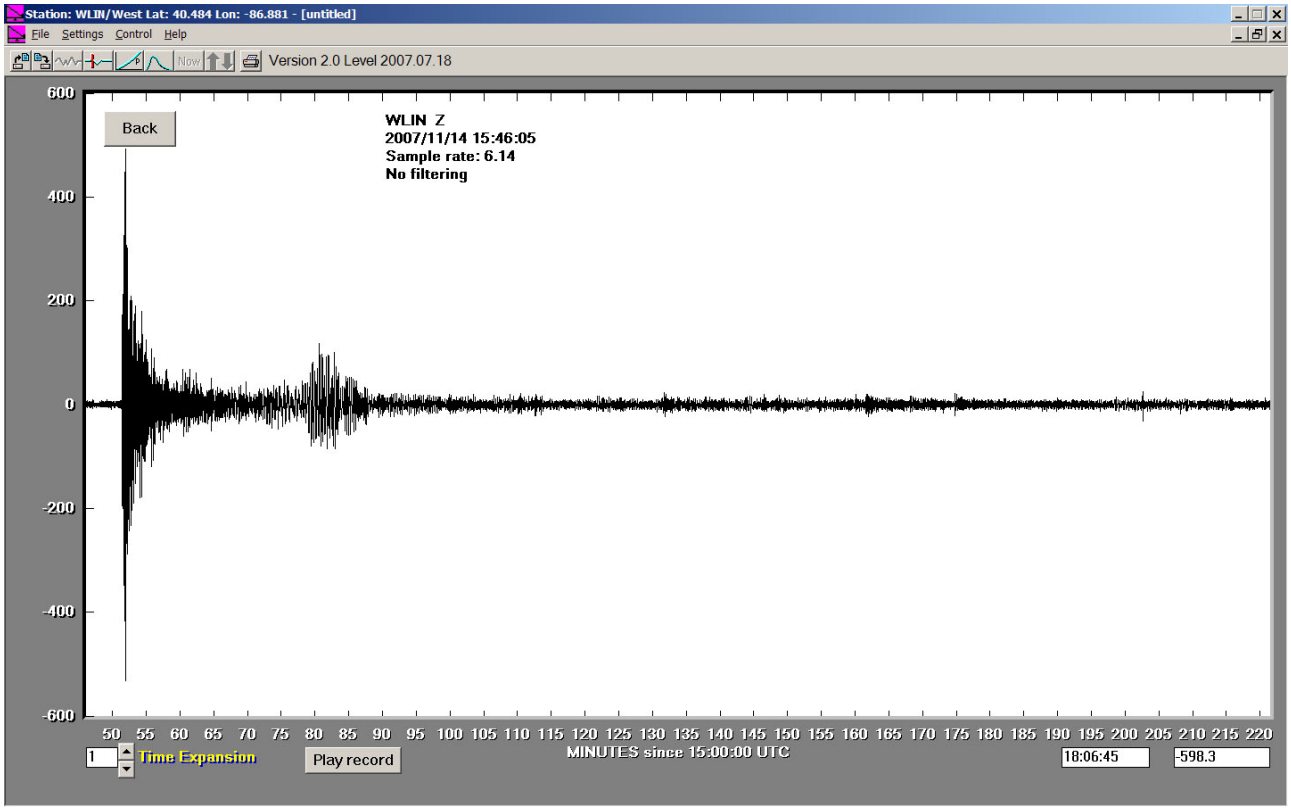

Figure 19. Three-hour seismogram record for the Northern Chile earthquake (http://web.ics.purdue.edu/~braile/edumod/as1lessons/filtering/0711141552WLINlong.sac).

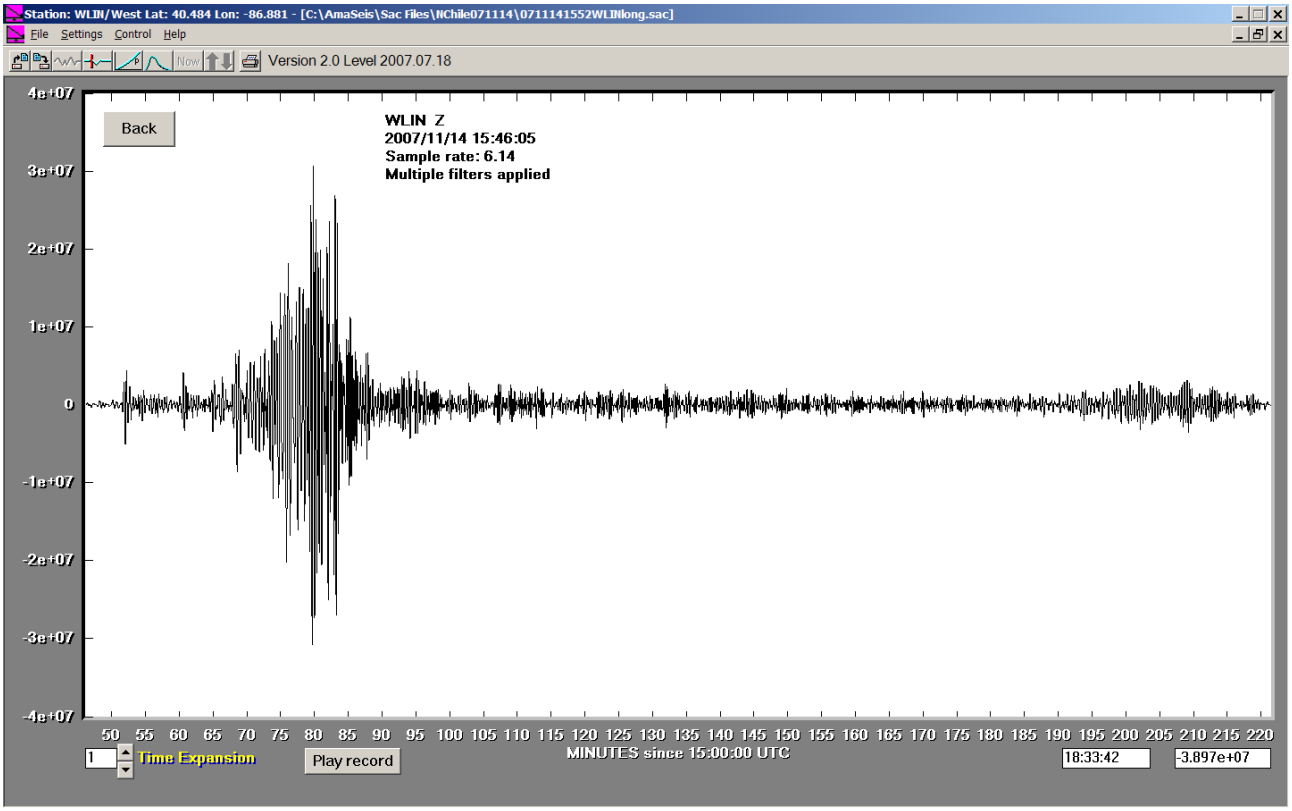

Figure 20. Long-period filtered (three times), three-hour seismogram of the M7.7 Northern Chile earthquake.

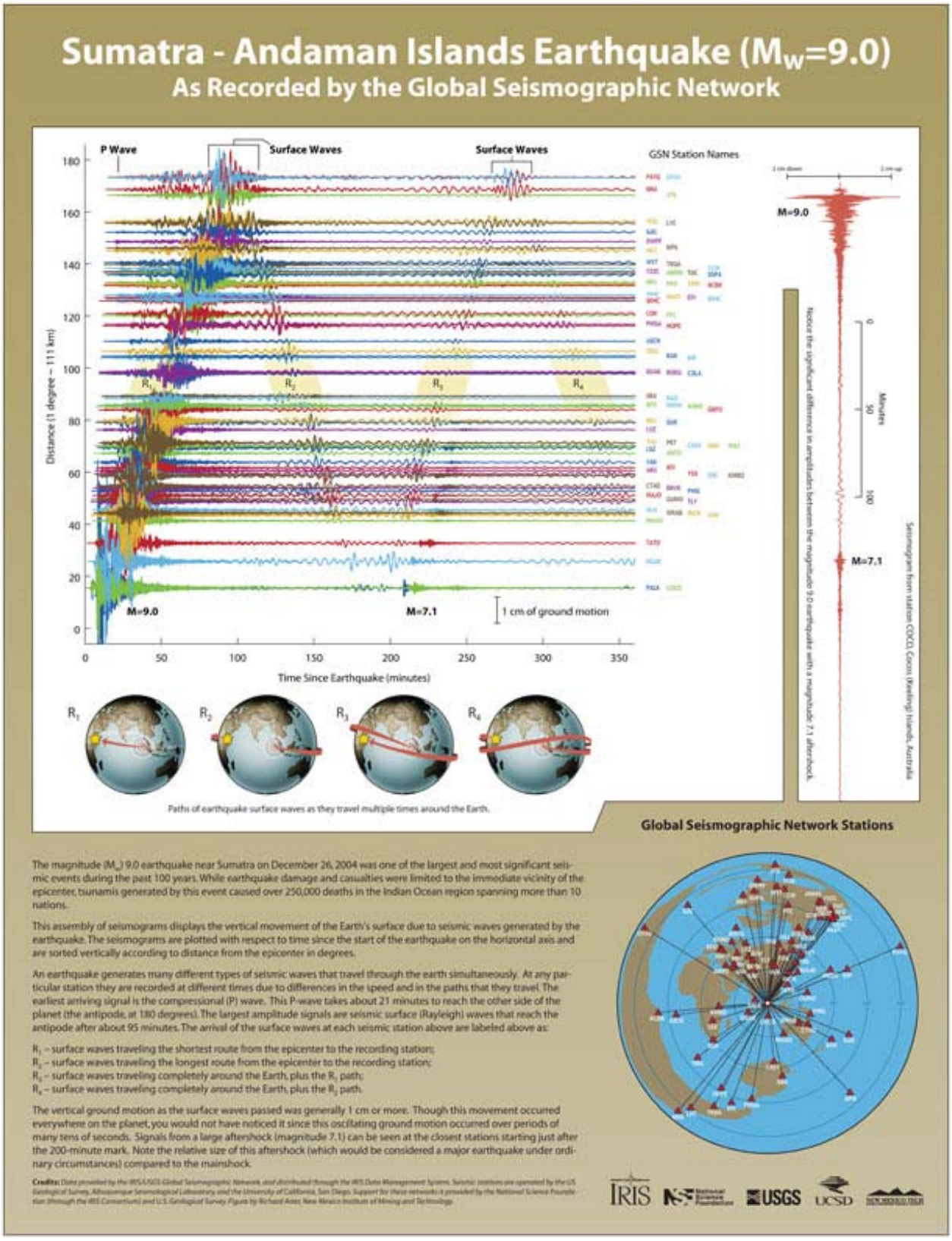

Figure 21. IRIS December 26, 2004 Sumatra earthquake poster (http://www.iris.edu/about/publications.htm#p).

8. Examples of High- and Low-Pass Filtering: The long period surface waves and high frequency arrival (PKPPKP) visible on the WLIN N. Chile seismogram provide an excellent opportunity to illustrate the effects of filtering. Figure 22 shows the original and filtered seismograms for these phases. Note that the high-pass filter enhances the high frequency energy associated with the PKPPKP arrival and effectively removes most of the low-frequency surface wave energy. Similarly, the low-pass filter enhances the surface wave energy and effectively removes most of the high frequency energy.

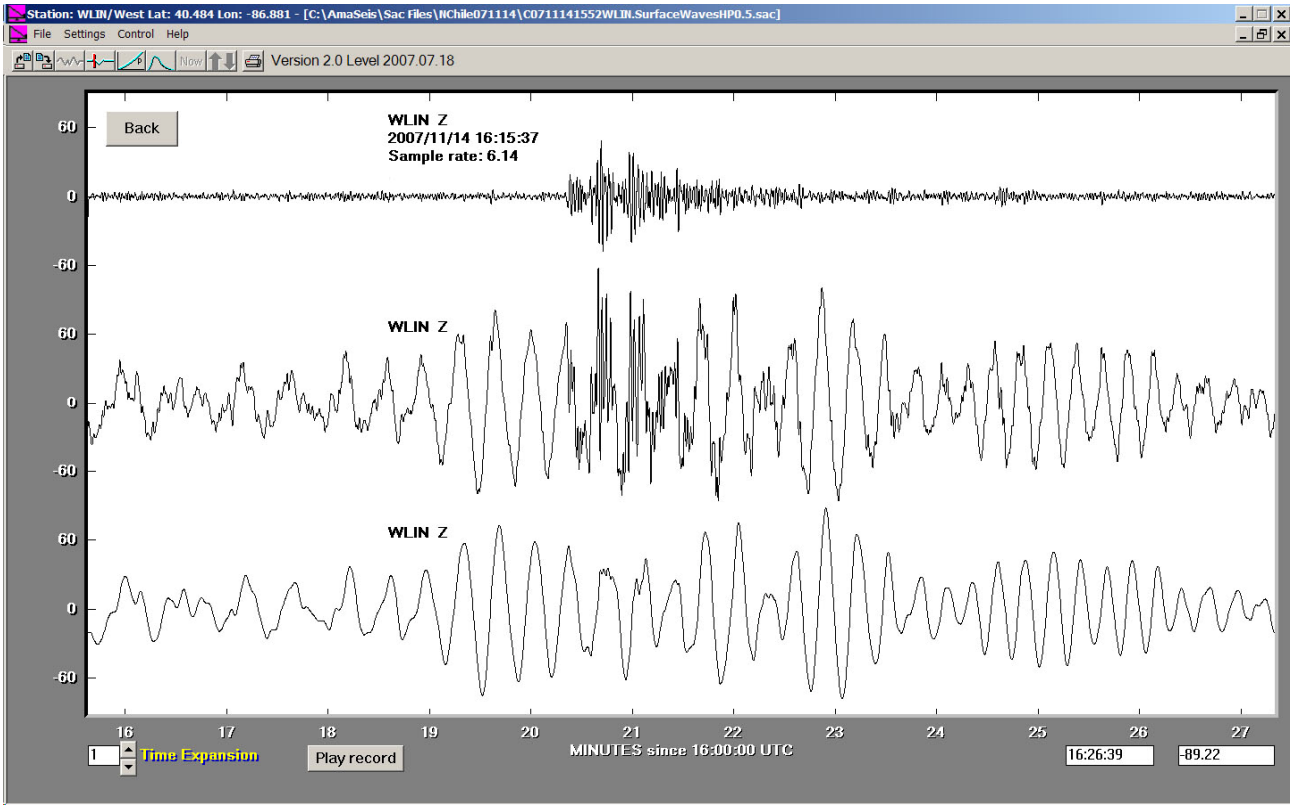

Figure 22. Example of seismogram filtering. Middle trace is original WLIN seismogram for the N. Chile earthquake showing the surface waves and "unusual" high frequency arrival (PKPPKP). Upper trace is the seismogram filtered with a high-pass filter (0.5 Hz cutoff frequency). Lower trace is the seismogram filtered with a low-pass filter (0.1 Hz cutoff frequency).

Surface waves recorded at teleseismic distances (greater than about 40 degrees), particularly surface waves that have traversed oceanic regions, often display a very sinusoidal (similar to a simple sine wave) character. An example is the surface wave energy from the November 27, 2007 Solomon Islands earthquake recorded on the WLIN seismograph (Figure 23). The seismogram was filtered twice with a low-pass filter to reduce the higher frequency energy and enhance the ~17 s period surface wave energy. As an additional example, the surface wave energy from the August 21, 2003 New Zealand earthquake recorded at the WLIN station was filtered twice with a low-pass filter. The filtered seismogram (Figure 24) has a very sinusoidal appearance but also illustrates a fundamental characteristic of surface waves – dispersion. As shown in Figure 24, the filtered seismogram clearly shows that the period (shown by the horizontal bars between two peaks) of the wave energy varies with time. Dispersion is the property that the velocity of wave propagation is different for different frequencies or periods. In this case, the longer period surface waves travel at faster speeds and thus arrive at the seismograph earlier.

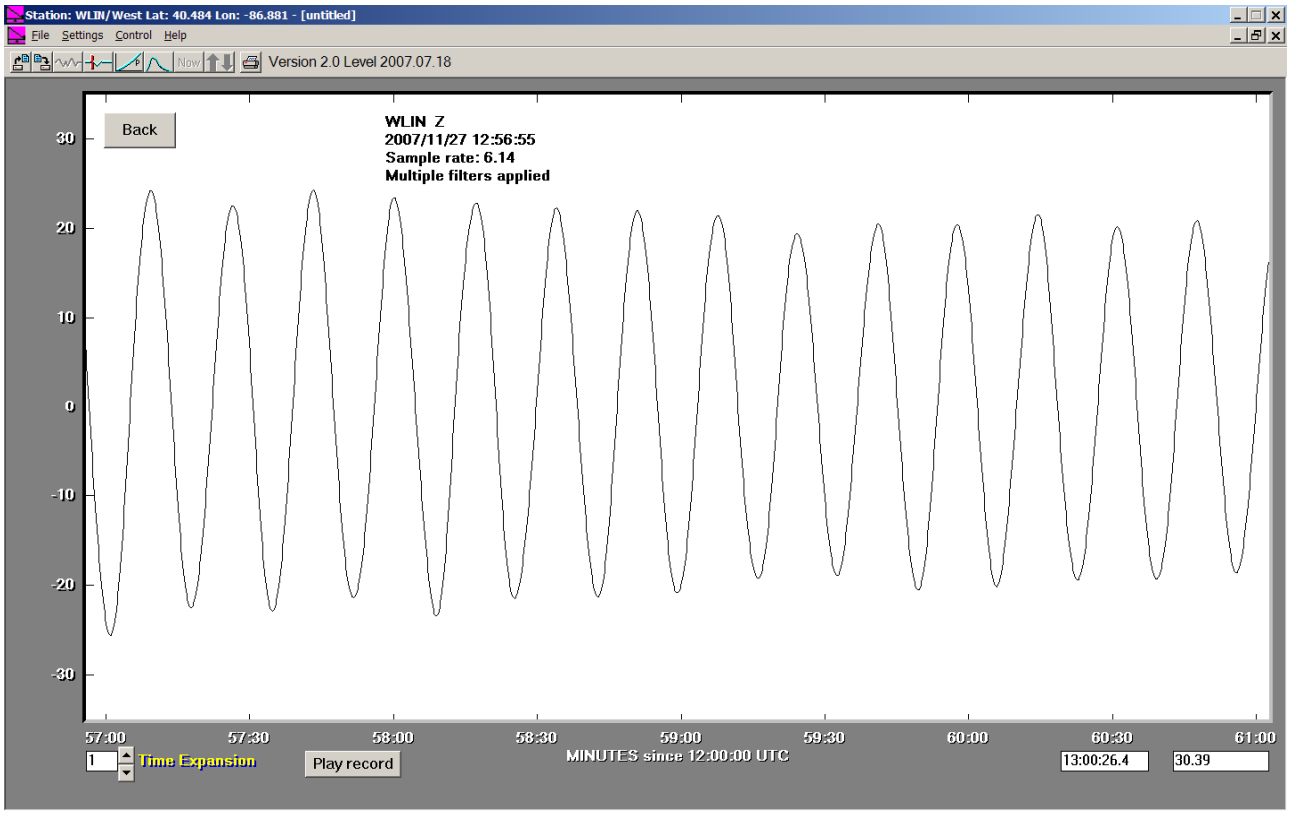

Figure 23. Surface waves from the November 27, 2007 Solomon Islands earthquake recorded on the WLIN AS-1 seismograph. The seismogram has been filtered twice with a low-pass filter (0.1 Hz cutoff frequency) to enhance the surface wave energy (http://web.ics.purdue.edu/~braile/edumod/as1lessons/filtering/0711271209WLIN.sac).

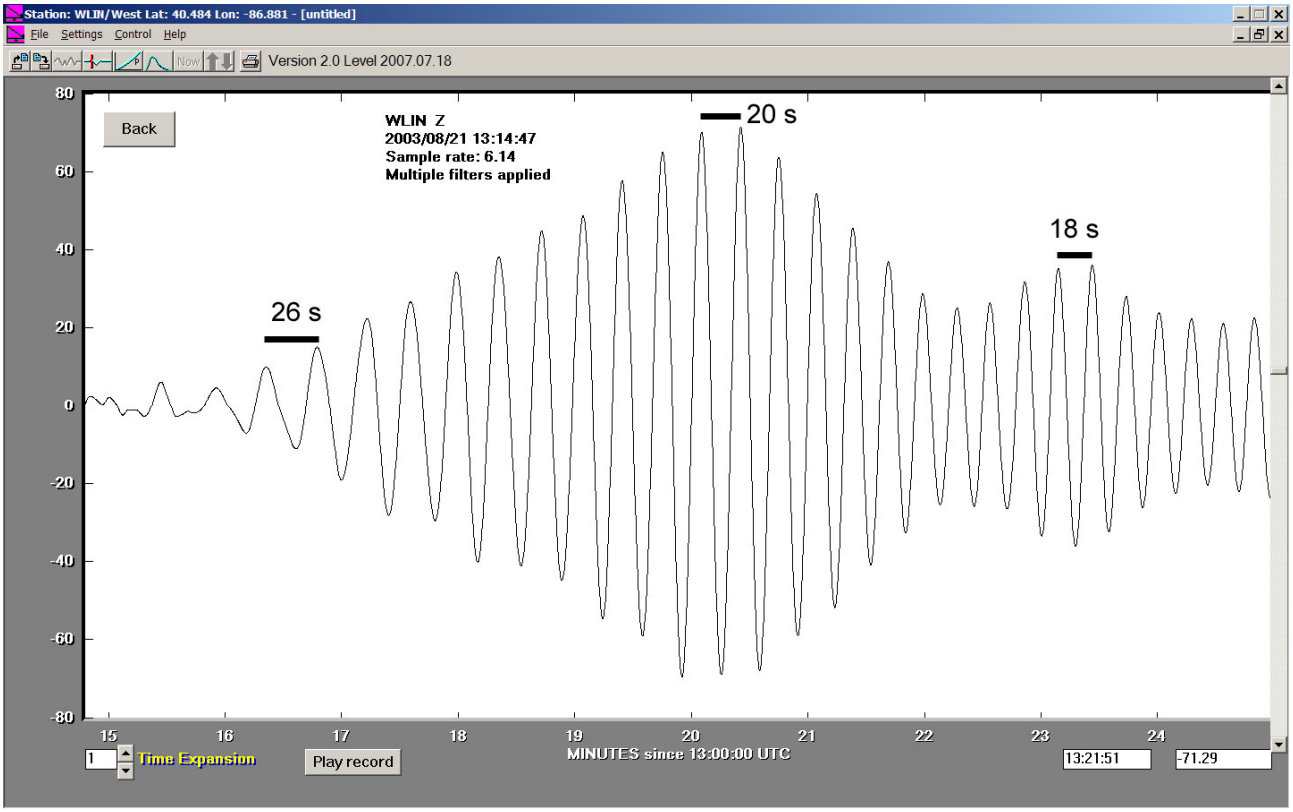

Figure 24. Surface waves from the August 21, 2003 New Zealand earthquake recorded on the WLIN AS-1 seismograph. The seismogram has been filtered twice with a low-pass filter (0.1 Hz cutoff frequency) to enhance the surface wave energy (http://web.ics.purdue.edu/~braile/edumod/as1lessons/filtering/0308211232WLIN.sac).

9. High-Pass Filtering to Identify Aftershocks: Moderate to large aftershocks are very common after major earthquakes. Sometimes, significant aftershocks occur within the first hour or so after a major event causing the P arrivals from the aftershocks to be recorded in the same time period as the surface waves for a distant event. An example is shown in Figure 25 for the November 15, 2006 M7.9 Kuril earthquake recorded at WLIN. After high-pass filtering the original seismogram, several prominent arrivals are visible on the filtered seismogram. Comparing arrival times of these events with the origin times of the aftershocks (the travel time from the epicentral area to WLIN is approximately 12 minutes) from the USGS list (Figure 26), we can identify at least six aftershocks. The aftershocks are numbered adjacent to the P arrival on the filtered seismogram and are listed in Figure 26. Arrivals labeled with a question mark on Figure 25 are uncertain as the possible corresponding events have small magnitude and would not be expected to be recorded at WLIN.

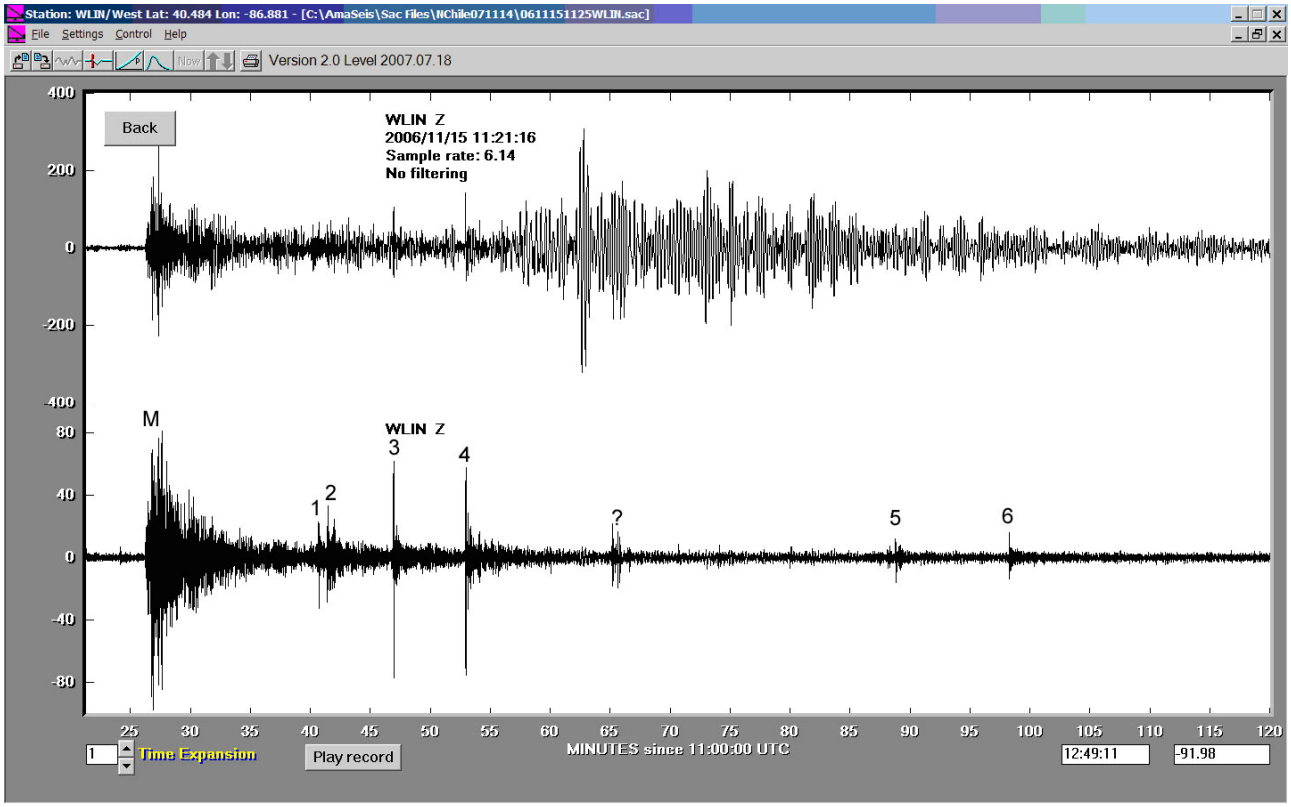

Figure 25. WLIN seismograms for the November 15, 2006 M7.9 Kuril earthquake. Upper trace is the original seismogram. Lower trace is the high-pass filtered (cutoff frequency = 0.5 Hz) seismogram (http://web.ics.purdue.edu/~braile/edumod/as1lessons/filtering/0611151125WLIN.sac). The P arrival for the main shock is labeled "M". The aftershocks are labeled with a number corresponding to the events listed in Figure 26.

	CATALOG SOURCE	DATE YEAR	MO	DA	ORIGIN TIME	***COORDINATES** LAT	LONG	DEPTH km		pP STD DEV	mb	OBS	*****MAGNITUDES**** Ms	OBS	OBS CONTRIBUTED VALUES
M	PDE	2006	11	15	111413.57 A	46.592	153.266	10	G	1.07	6.5	99	7.8Z	99	8.30MwGCMT
															7.90MwGS
	PDE	2006	11	15	112306.92*B	46.301	154.610	10	G	1.47	5.6	29			
	PDE	2006	11	15	112429.86 A	46.270	154.520	10	G	0.94	5.6	56			
	PDE	2006	11	15	112457.49*B	47.770	153.179	10	G	0.96	5.5	15			
	PDE	2006	11	15	112509 A	47.518	152.647	10	G	1.38	6.0	99			
1	PDE	2006	11	15	112838.46 A	46.086	154.100	10	G	0.84	6.0	99			
2	PDE	2006	11	15	112922.79 A	46.371	154.475	10	G	1.07	6.2	99			
	PDE	2006	11	15	113323.80 A	46.862	153.731	10	G	1.07	5.5	33			
3	PDE	2006	11	15	113458.13 A	46.652	155.305	10	G	0.84	6.4	99			
	PDE	2006	11	15	114003.87*B	47.673	151.525	10	G	1.10	5.3	15			
4	PDE	2006	11	15	114055.05 A	46.483	154.726	10	G	0.90	6.4	99			6.70MwGCMT
	PDE	2006	11	15	114804.23*B	44.104	154.700	10	G	1.45	5.5	21			
	PDE	2006	11	15	115255.86*B	47.362	154.411	10	G	1.39	5.0	10			
	PDE	2006	11	15	120917.43 A	47.323	155.361	10	G	0.93	5.4	99			
	PDE	2006	11	15	121523.80 A	46.301	154.407	10	G	0.88	5.3	74			
5	PDE	2006	11	15	121605.54 A	47.111	154.417	10	G	1.39	5.7	84			
5	PDE	2006	11	15	121644.15 A	46.195	154.668	10	G	0.82	5.9	99			
	PDE	2006	11	15	122304.07 A	46.789	153.395	10	G	1.12	5.0	39			
6	PDE	2006	11	15	122615.76 A	47.421	153.861	10	G	0.79	5.7	99			
	PDE	2006	11	15	122821.33 A	47.055	155.526	10	G	0.89	5.5	65			

Figure 26. Table of earthquake information for the November 15, 2006 M7.9 Kuril earthquake and aftershocks (USGS PDE catalog available from the earthquake search tool: http://neic.usgs.gov/neis/epic/epic.html). Identification of the main shock and aftershock numbers have been added to the Table.

10. Filtering the AmaSeis Helicorder 24-Hour Display: To reduce some of the background noise and enhance the signals from distant earthquakes, John Lahr suggests (http://jclahr.com/science/psn/as1/filtering/index.html) trying the band-pass filter option on the AmaSeis display (helicorder). The original, unfiltered data are stored in the computer files, so one can turn the filter on or off and only the screen image is changed. An example is given in Figure 27. Notice that in the filtered signal, the high-frequency noise and microseisms are reduced and the long-period energy, especially the surface waves, are enhanced so that the earthquake signal is more visible.

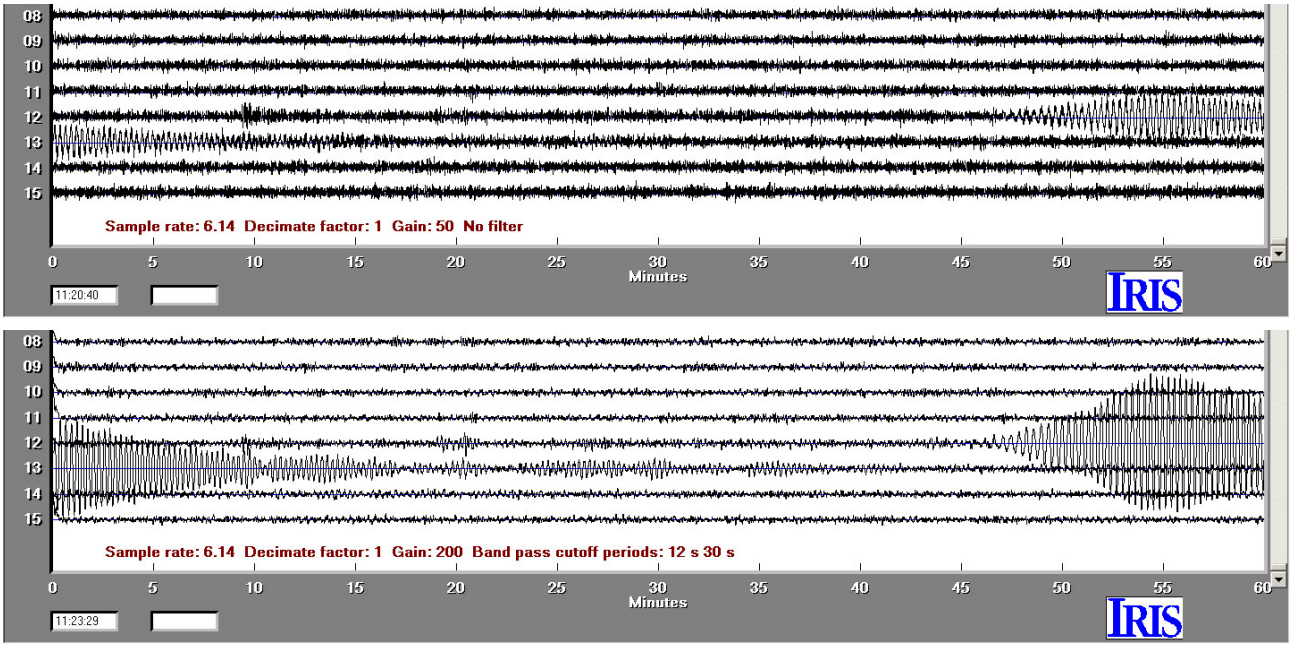

Figure 27. Partial helicorder (24-hour screen) displays using AmaSeis for the November 27, 2007 M6.6 Solomon Islands earthquake recorded at the WLIN AS-1 station. Upper image shows the one-hour traces including the earthquake record with no filtering and a gain of 50. Lower image shows the one-hour traces including the earthquake record with filtering (band-pass filter 12-30 second period by setting the Helicorder options in the Settings pull-down menu in AmaSeis) turned on and a gain of 200.

11. Suggestions for Additional Activities and Demonstrations of Filtering and Interpretation of Seismograms – See What You can Discover! Some suggestions for further exploration of seismograms and filtering are provided below. Some additional resources and information for the AmaSeis software, seismograph analysis and filtering are contained in the Using AmaSeis tutorial, the Interpreting Seismograms tutorial and in John Lahr's web page on filtering:
http://web.ics.purdue.edu/~braile/edumod/as1lessons/UsingAmaSeis/UsingAmaSeis.htm
http://web.ics.purdue.edu/~braile/edumod/as1lessons/InterpSeis/InterpSeis.htm
http://jclahr.com/science/psn/as1/filtering/index.html. Information on the seismograms in sections 8, 9, 10 and 11 is contained in the Table in Figure 28.

	A	B	C	D	E	F	G	H	I	J	K	L	M	N	O	P
1	Earthquake List - Events recorded, WLIN AS-1 Seismograph (40.484N, 86.881W, 205 m), West Lafayette, Indiana (L. Braile)															
2	DATE	TIME(GMT)	LAT	LON	DEP.	USGS	USGS	USGS	USGS	AS-1	AS-1	AS-1	Calc. Dist	AS-1 Dist	Location	Comments
3	YY/MM/DD	HR:MN:SS	Deg.	Deg.	(km)	mb	MS	Mw	mbLg	mb	MS	mbLg	Deg.	Deg.		X = lost data
4	01/01/26	3:03:19	41.990	-80.830	5				4.2			4.1	4.800	4.9	Ohio	Good S-P
5	01/06/23	20:33:14	-16.265	-73.641	33	6.7	8.2	8.4		6.5	7.7		57.740		Near coast of Peru	Good complete seismogram
6	03/08/21	12:12:50	-45.154	167.179	33	6.5	7.5	7.2			7.6		127.240		S. Is. New Zealand	Excellent, dispersed Rayleigh
7	05/06/13	22:44:34	-19.934	-69.028	117	6.9		7.8		7.5			62.360	62.6	Tarapaca, Chile	
8	06/11/15	11:14:14	46.592	153.266	10	6.5	7.8	7.9		6.7	7.8		78.090		Kuril Islands	Aftershocks (HP filter)
9	07/08/15	23:40:59	-13.354	-76.509	39	6.7	7.9	8.0		6.3	7.3		54.420	54.5	Near coast of C. Peru	3rd M8+ event of 2007
10	07/11/27	11:50:02	-11.022	162.166	42	5.8	6.7	6.6		6.1	6.8		112.990		Solomon Islands	
11																

Figure 28. Table of earthquake information for seismograms used in Sections 8, 9, 10 and 11.

a. Perform one or more of the filtering and analysis processes contained in sections 4 through 10 using the seismograms provided.

b. High pass filter (0.5 Hz cutoff frequency; or 2 s cutoff period) the June 13, 2005 M7.8 Tarapaca, Chile earthquake seismogram and see if a PKPPKP arrival is present. Notice the difference in character of the filtered and unfiltered seismograms. Use the Table in Figure 12 or online calculations of distance and arrival time of phases (http://neic.usgs.gov/neis/travel_times/) to compare the observed and calculated PKPPKP minus P time. The seismogram is available at: http://web.ics.purdue.edu/~braile/edumod/as1lessons/filtering/0506132254WLIN.sac.

c. Apply the long period filter to the Tarapaca, Chile seismogram (from b., above) and use the travel time curve tool in AmaSeis to estimate the distance using the S minus P method (the distance can be estimated most accurately by extracting about 30 seconds of the seismogram from just before the P arrival to the middle of the surface wave energy). How does the estimated distance compare to the calculated distance from the Table in Figure 28?

d. Open the Tarapaca, Chile seismogram (from b., above) in AmaSeis. Note the weak surface wave energy and high frequency arrival at a time of about 23 hours and 24 minutes (23:24). Extract a short portion of the seismogram (about 5 minutes long) that contains the surface wave and high frequency arrival (PKPPKP). Apply a low-pass filter (cutoff period of 10 s) to the extracted seismogram. Notice the difference between the original and filtered seismograms. Measure the period of the surface wave energy using the arrival times for the cursor position from two successive peaks of the surface wave energy (should be about 20 s period). Because this was a deeper focus earthquake (117 km), the surface waves are weaker and are not used for calculating magnitude.

e. Use the November 11, 2006 M7.9 Kuril Islands earthquake seismogram to calculate the mb and MS magnitudes. You can use the magnitude calculator in AmaSeis or the online AS-1 Magnitude Calculator (http://web.ics.purdue.edu/~braile/edumod/MagCalc/MagCalc.htm). Compare your calculated magnitudes with those listed in the Table in Figure 28. The seismogram is available at: http://web.ics.purdue.edu/~braile/edumod/as1lessons/filtering/0611151125WLIN.sac.

f. High pass filter (0.5 Hz cutoff frequency; or 2 s cutoff period) the June 23, 2001 M8.4 Peru earthquake seismogram. Try to identify as many aftershocks as you can on the seismogram by comparing origin times from the USGS earthquake list given in Figure 29. The travel time from the epicentral area to the WLIN station is about 10.5 minutes. The seismogram is available at: http://web.ics.purdue.edu/~braile/edumod/as1lessons/filtering/0106232043WLIN.sac

CATALOG SOURCE	DATE YEAR	MO	DA	ORIGIN TIME	***COORDINATES** LAT	LONG	DEPTH km		pP STD DEV	*****MAGNITUDES**** mb	OBS	Ms	OBS	CONTRIBUTED VALUES
PDE	2001	06	23	203314.13	-16.264	-73.641	33	N	1.05	6.7	99	8.2Z	99	8.40MwHRV 8.30MwGS
PDE	2001	06	23	205452.27?	-16.569	-73.728	33	N	1.38	5.4	11			
PDE	2001	06	23	205607.21	-17.400	-72.166	33	N	0.99	5.8	39			
PDE	2001	06	23	210539.17	-17.840	-71.348	33	N	1.04	5.8	36			
PDE	2001	06	23	211614.87*	-17.322	-71.956	33	N	0.92	5.1	15			
PDE	2001	06	23	211910.75	-17.047	-73.523	33	N	0.77	5.2	18			
PDE	2001	06	23	212208.98*	-17.284	-72.237	33	N	1.38	5.4	11			
PDE	2001	06	23	212735.71	-17.181	-72.641	33	N	0.92	6.1	84			
PDE	2001	06	23	213849.89	-17.115	-72.373	33	N	1.18	5.3	68			
PDE	2001	06	23	214134.27*	-17.720	-71.054	33	N	0.99	5.0	4			
PDE	2001	06	23	215453.81	-17.202	-72.632	33	N	1.05	5.1	44			
PDE	2001	06	23	215927.34	-16.756	-73.819	33	N	1.07	5.4	28			
PDE	2001	06	23	222439.52	-16.645	-73.606	33	N	0.88	5.7	78			
PDE	2001	06	23	223237.28	-17.602	-72.646	33	N	1.02	5.5	60			
PDE	2001	06	23	231000.99	-16.767	-73.632	33	N	1.20	5.9	97			
PDE	2001	06	23	234456.02	-16.751	-73.723	33	N	0.83	5.4	72			
PDE	2001	06	23	234913.88	-17.849	-71.579	33	N	0.87	5.6	83			

Figure 29. Table of earthquake information for the June 23, 2001 M8.4 Peru earthquake and aftershocks (USGS PDE catalog available from the earthquake search tool: http://neic.usgs.gov/neis/epic/epic.html).

g. Apply a high-pass filter (2 s cutoff period) twice to the January 26, 2001 M4.2 Ohio earthquake seismogram. In this case the high-pass filter enhances the P and S arrivals. The background noise is primarily microseisms of about 4 second period. Compare the characteristics of the filtered and unfiltered seismograms. Use the travel time curve tool in AmaSeis to estimate the distance using the S minus P method (the S arrival, before the Lg arrival, is recognized by large amplitude and change to longer period). Compare with the calculated distance from the Table in Figure 28. Next, calculate the mbLg magnitude. You can use the magnitude calculator in AmaSeis or the online AS-1 Magnitude Calculator (http://web.ics.purdue.edu/~braile/edumod/MagCalc/MagCalc.htm). Compare your calculated magnitudes with those listed in the Table in Figure 28. The seismogram is available at: http://web.ics.purdue.edu/~braile/edumod/as1lessons/filtering/0101260305WLIN.sac.

h. High pass filter (0.5 Hz cutoff frequency; or 2 s cutoff period) the August 15, 2007 M8.0 Peru earthquake seismogram. Try to identify as many aftershocks as you can on the seismogram by comparing origin times from the USGS earthquake list that you can obtain with the earthquake search tool from http://neic.usgs.gov/neis/epic/epic.html (select expanded file format; search on the dates 8/15-8/16 with magnitude range 5 to 10). The travel time from the epicentral area to the WLIN station is about 9.5 minutes. The seismogram is available at: http://web.ics.purdue.edu/~braile/edumod/as1lessons/filtering/0708152350WLIN.sac.

i. We have seen that seismic signals from earthquakes have interesting frequency characteristics that can be analyzed and interpreted using filtering, but we have not examined the background noise that is always visible on the seismograph record. In this activity, we will use two noise samples to analyze the background noise level, frequency content of the noise, and the characteristics of microseisms. Background noise is caused by environmental conditions such as high winds and ocean waves and oscillations in coastal areas (microseisms), local human effects (machinery, traffic, people walking), and distant small earthquakes and low level shaking from recent large earthquakes long after the main seismic signals have passed. Two screen displays of background noise are shown in Figure 30. The first display is during a very quiet time period while the second

display is during a very noisy time period. A sample of about 20 minutes long of the noise (Noise1) in the first example (quiet background noise) has been extracted as a seismogram. Similarly, a sample of about 20 minutes long of the noise (Noise2) in the second example (large background noise) has been extracted as a seismogram. For each seismogram noise sample, apply a 1 Hz low-pass filter to the data (to reduce the highest frequency, relatively erratic oscillations in the noise seismograms. Note the noise level (amplitude, in digital units) and appearance of the noise in the two samples. Extract about a 2 minute section of the filtered noise samples and measure the period between two successive peaks. Open the seismograms again and filter them. Now use the Fourier transform tool in AmaSeis to calculate the spectrum that displays the relative amounts of amplitudes (or energy) in the signal at various frequencies. Compare the spectrum for each noise sample. The noise in the second example (Noise2) is primarily caused by microseisms that are commonly generated by wave action and oscillations associated with storms along the east coast of North America. The microseisms, with a characteristic period of about 4-6 seconds, propagate very efficiently through eastern North America and are therefore very visible on the WLIN seismograph record. For more information on the Fourier transform, see Section 3.9 of the Using AmaSeis tutorial (http://web.ics.purdue.edu/~braile/edumod/as1lessons/UsingAmaSeis/UsingAmaSeis.htm) and John Lahr's filtering web page (http://jclahr.com/science/psn/as1/filtering/index.html). The seismograms are available at:
http://web.ics.purdue.edu/~braile/edumod/as1lessons/filtering/0707080220WLIN.Noise1.sac
http://web.ics.purdue.edu/~braile/edumod/as1lessons/filtering/0711032324WLIN.Noise2.sac.

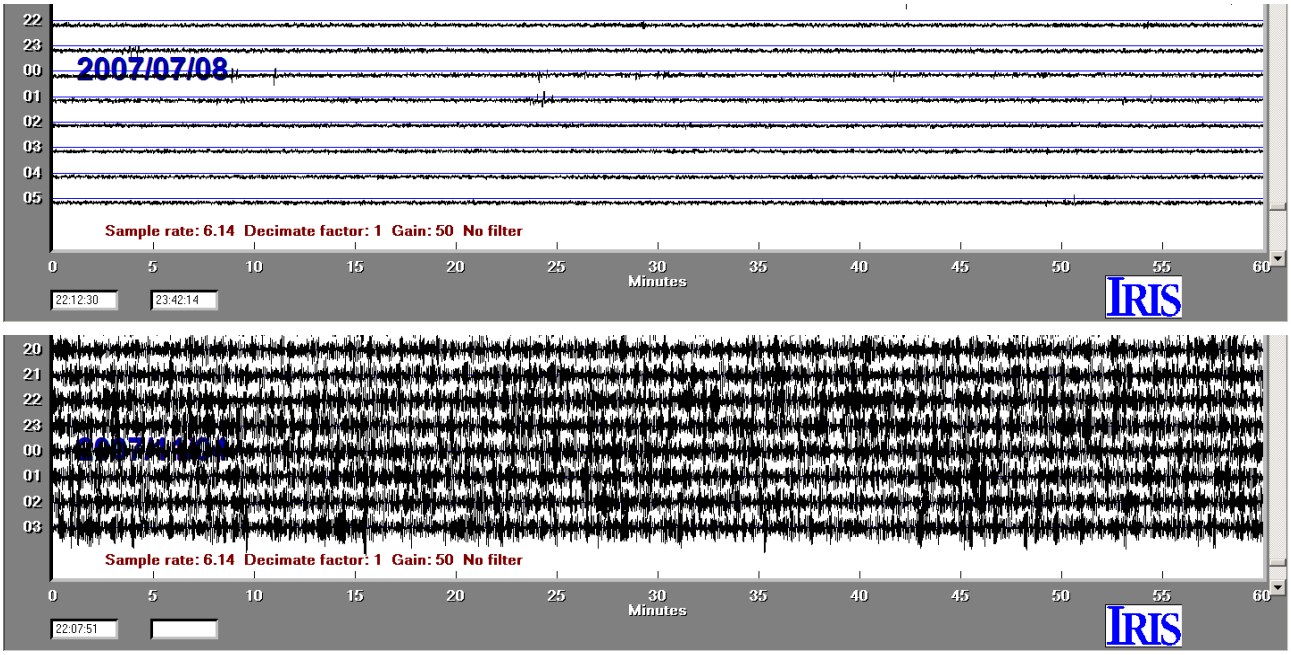

Figure 30. Partial helicorder (24-hour screen) displays using AmaSeis for two time periods during the year 2007 recorded at the WLIN AS-1 seismograph station. Upper image shows the one-hour traces of background noise from 22:00 on July 7 to 06:00 on July 8. Lower image shows the one-hour traces of background noise from 20:00 on November 3 to 04:00 on November 4. No filter has been applied and the gain is 50 for both displays.